

hep-ph/9511407  
TUM-HEP-224/95  
TUM-T31-90/95  
November 1995

## Higgs Sector Renormalization Group in the $\overline{\text{MS}}$ and OMS Scheme: The Breakdown of Perturbation Theory for a Heavy Higgs

Ulrich Nierste\* and Kurt Riesselmann†

*Physik-Department T30, Technische Universität München,  
James-Frank-Straße, 85747 Garching b. München, Germany*

### Abstract

We discuss different aspects of the Higgs self-interaction in the  $\overline{\text{MS}}$  and the on-mass-shell (OMS) scheme. The running coupling  $\lambda(\mu)$  is investigated in great detail. The three-loop coefficient of the  $\beta$ -function in the OMS scheme is derived, and the three-loop running coupling is calculated. The breakdown of perturbation theory for large Higgs masses  $M_H$  is analyzed in three physical observables for which two-loop results are known. Requiring the dependence on the renormalization scale to diminish order-by-order in  $\lambda$ , we find that perturbation theory breaks down for  $M_H = \text{O}(700 \text{ GeV})$  in Higgs decays. Similarly,  $M_H$  must be smaller than  $\text{O}(400 \text{ GeV})$  for perturbatively calculated cross sections to be trustworthy up to cm energies of  $\text{O}(2 \text{ TeV})$ . If the Higgs sector shall be perturbative up to the GUT scale, the Higgs must be lighter than  $\text{O}(150 \text{ GeV})$ . For the two-loop observables examined, the apparent convergence of the perturbation series is better in the OMS scheme than in the  $\overline{\text{MS}}$  scheme.

PACS numbers: 14.80.Bn, 11.10.Hi, 11.10.Jj, 11.15.Bt, 11.15.Ex

Typeset using REVTeX

---

\*Electronic address: nierste@physik.tu-muenchen.de

†Electronic address: kurtr@physik.tu-muenchen.de

## I. INTRODUCTION

One of the least tested sectors of the Standard Model of elementary particle physics is the Higgs sector generating the masses of all particles via the mechanism of spontaneous symmetry breaking. This mechanism implies that the self-coupling  $\lambda$  of the Higgs particle is proportional to the square of its mass,  $M_H$ . Hence a heavy Higgs particle may cause the breakdown of perturbation theory in  $\lambda$ .

When calculating decay rates or cross sections beyond the tree level term of the perturbation series one must specify the *renormalization scheme* to define the coupling constants and the particle masses appearing in the analytic expressions. In the Higgs sector one usually adopts the *on-mass-shell scheme* (OMS): Here the squared mass coincides with the physical pole of the propagator, the vacuum expectation value  $v = 246$  GeV of the Higgs field is renormalized such as to cancel tadpole contributions, and the coupling is chosen to satisfy

$$\lambda_{\text{OMS}} = \frac{M_H^2}{2v^2} = \frac{G_F M_H^2}{\sqrt{2}} \quad (1.1)$$

to all orders in perturbation theory.<sup>1</sup> Here  $G_F$  is the Fermi constant. When discussing the perturbation series of physical observables one must first distinguish processes involving two largely separated mass scales from those containing only one scale,  $M_H$ . Prototypes of the first species are cross sections at LHC energies. They contain potentially large logarithmic terms  $\lambda \ln(\sqrt{s}/M_H)$  with  $\sqrt{s}$  being the energy of the process. These terms may spoil the smallness of radiative corrections. Yet they can be summed to all orders in perturbation theory with the help of *renormalization group* (RG) methods. The corresponding equation in the OMS is the *Callan-Symanzik equation*, which can be solved in the limit of large  $\sqrt{s}$  when all particle masses can be neglected. The second kind of physical observables are one-scale processes. Examples are two-body decay rates of the Higgs particle into (almost) massless particles. We will see in the following that RG methods are also a useful tool to judge the accuracy of perturbative results in these cases.

Due to (1.1) the use of the OMS appears natural, because  $\lambda_{\text{OMS}}$  is directly related to physical observables. Yet it is also useful to consider mass independent renormalization schemes, the most prominent example being the  $\overline{\text{MS}}$ -scheme. The reasons are the following:

- i) Mass independent schemes allow for an exact solution of the RG equations, i.e. mass effects can be systematically included.
- ii) The analysis of scheme dependences provides a test of the reliability of perturbation theory since the results obtained to order  $\lambda^n$  in different schemes formally differ by terms of order  $\lambda^{n+1}$ .
- iii) Results obtained in mass independent schemes involve an arbitrary parameter, the *renormalization scale*  $\mu$ . For perturbation theory to work it is necessary that the dependence of the result on  $\mu$  diminishes order by order in perturbation theory. We will use this fact extensively in the discussion of the breakdown of perturbation theory.

---

<sup>1</sup>We consistently neglect all gauge coupling corrections.  $\Delta r$  is hence taken to be zero.

The paper is organized as follows: In the following section we discuss the running coupling constant in the two-loop approximation. In Sect. III we give the two-loop relation between the quartic Higgs coupling in the OMS and the  $\overline{\text{MS}}$  scheme. We calculate the three-loop OMS coefficient of the  $\beta$  function as well as the coefficients of the leading and next-to-leading logarithms. Subsequently, we investigate the scheme and scale dependence of two-loop physical observables using the three-loop running coupling. Special attention is paid to the breakdown of perturbation theory for heavy Higgs masses. We start by examining the bosonic and fermionic Higgs decay widths (Sect. IV). Finally, we look at scattering processes which involve the longitudinally polarized gauge bosons  $W_L^\pm$  and  $Z_L$ . These scattering processes give the most stringent bounds on a perturbative Higgs mass (Sect. V).

## II. PERTURBATIVE RUNNING COUPLING AT DIFFERENT ORDERS

We first discuss the coupling constant  $\lambda(\mu)$ , whose running is encoded in the  $\beta$ -function. To three loops, the beta function of the Higgs quartic coupling is defined as

$$\beta \equiv \mu \frac{d\lambda}{d\mu} \equiv \frac{\beta_0}{16\pi^2} \lambda^2 + \frac{\beta_1}{(16\pi^2)^2} \lambda^3 + \frac{\beta_2}{(16\pi^2)^3} \lambda^4 + \mathcal{O}(\lambda^5). \quad (2.1)$$

We neglect all contributions from gauge and Yukawa couplings. This is an excellent approximation for large values of  $\lambda$ . To two loops the coefficients are [1]

$$\beta_0 = 24, \quad \beta_1 = -13\beta_0 = -312. \quad (2.2)$$

The three-loop coefficient  $\beta_2$  is scheme dependent. We restrict the discussion of this section to the scheme independent two-loop results and return to  $\beta_2$  in Sect. III.

Equation (2.1) is valid in any mass independent scheme with  $\mu$  being the renormalization scale accompanying the coupling constant in the Lagrangian. In the OMS scheme, the Callan-Symanzik equation describes the response of some Green's function to the scaling of its external momenta according to  $p_i \rightarrow \mu/\mu_0 \cdot p_i$  which is related to the corresponding scaling of the coupling given by Eq. (2.1). The values of  $\beta_0$  and  $\beta_1$  are scheme independent, so that we don't choose a specific renormalization scheme until later. The determination of  $\lambda(\mu)$  proceeds in two steps: First at some initial scale  $\mu_0 \approx M_H$  the coupling  $\lambda(\mu_0)$  is obtained from (1.1) or an equivalent relation, if the scheme under consideration is not the OMS scheme.<sup>2</sup> Then (2.1) is solved for  $\lambda(\mu) \equiv \lambda[\lambda(\mu_0), \mu/\mu_0]$ . The question whether perturbation theory works in a specific physical process therefore depends on the two parameters  $\lambda(\mu_0)$  and  $\mu/\mu_0$ , which are related to the physical parameters  $M_H$  and the energy  $\sqrt{s}$  of the process. The cause of a possible breakdown of perturbation theory is twofold: First, the larger the Higgs mass,  $M_H$ , the larger is  $\lambda(\mu_0)$  due to

---

<sup>2</sup>For the  $\overline{\text{MS}}$  scheme, the expression for  $\lambda(\mu_0)$  is derived in section III, see Eq. (3.3).

(1.1). Second, the resummation of possibly large logarithms,  $\ln(\sqrt{s}/M_H)$ , introduces the running coupling  $\lambda(\mu)$  with  $\mu \approx \sqrt{s}$ , and  $\lambda(\mu)$  increases for increasing  $\mu \approx \sqrt{s}$ .

Defining  $\lambda$  at some initial scale  $\mu_0$ , the solution of (2.1) yields  $\lambda(\mu)$  at any other scale  $\mu$ . The expansion of  $\lambda(\mu)$  around  $\lambda(\mu_0)$  shows that  $\lambda(\mu)$  resums powers of the logarithm  $\ln(\mu/\mu_0)$  multiplied by powers of  $\lambda(\mu_0)$ . The coefficients of the leading logarithms (LL),  $\lambda^{n+1}(\mu_0) \ln^n(\mu/\mu_0)$ , depend only on  $\beta_0$ , those of the next-to-leading logarithms (NLL) depend on both  $\beta_1$  and  $\beta_0$ , and so on. We will give these coefficients explicitly later. The first point we want to stress is that beyond the one-loop approximation there are several different solutions of Eq. (2.1) due to the truncation of the perturbation series. All of them agree to the order at which the perturbative series of the beta function, (2.1), is truncated, but they differ by terms of the neglected order. For a viable perturbative treatment, these higher-order differences should be negligible. We now look at four different solutions for the running coupling  $\lambda(\mu)$ .

Setting simply the coefficients of the neglected terms in (2.1) equal to zero and integrating the remaining expressing exactly, we obtain an implicit equation for  $\lambda(\mu)$ :

$$\frac{\lambda(\mu_0)}{\lambda(\mu)} = 1 - \beta_0 \hat{\lambda}(\mu_0) \ln \left( \frac{\mu}{\mu_0} \right) + \frac{\beta_1}{\beta_0} \hat{\lambda}(\mu_0) \ln \left( \frac{(\beta_0 + \beta_1 \hat{\lambda}(\mu)) \hat{\lambda}(\mu_0)}{(\beta_0 + \beta_1 \hat{\lambda}(\mu)) \hat{\lambda}(\mu)} \right) \quad (2.3)$$

in the NLL approximation, and

$$\begin{aligned} \frac{\lambda(\mu_0)}{\lambda(\mu)} = & 1 - \beta_0 \hat{\lambda}(\mu_0) \ln \left( \frac{\mu}{\mu_0} \right) + \frac{\beta_1}{\beta_0} \hat{\lambda}(\mu_0) \ln \left( \frac{\hat{\lambda}(\mu_0)}{\hat{\lambda}(\mu)} \right) \\ & + \frac{\beta_0 \beta_2 \hat{\lambda}(\mu_0)}{\lambda_b - \lambda_a} \left[ \frac{1}{\lambda_b^2} \ln \frac{\lambda_b - \hat{\lambda}(\mu)}{\lambda_b - \hat{\lambda}(\mu_0)} - \frac{1}{\lambda_a^2} \ln \frac{\lambda_a - \hat{\lambda}(\mu)}{\lambda_a - \hat{\lambda}(\mu_0)} \right] \end{aligned} \quad (2.4)$$

with

$$\lambda_{a/b} = -\frac{\beta_1}{2} \pm \frac{1}{2} \sqrt{\beta_1^2 - 4\beta_0\beta_2}$$

in the next-to-next-to-leading log (NNLL) approximation.<sup>3</sup> Here (2.3) is the two-loop result published previously [2]. In (2.3) and (2.4) the useful abbreviation  $\hat{\lambda} = \lambda/(16\pi^2)$  has been used. To obtain  $\lambda(\mu)$  one has to solve (2.3) or (2.4) by numerical methods. Direct numerical integration of the original equation, (2.1), yields the same result for  $\lambda(\mu)$ . Let us call this form the *naive* solution. It would be the exact result if the neglected coefficients of the  $\beta$ -function were really identical to zero. Yet (2.3) and (2.4) contain logarithmic terms belonging to the neglected higher orders of RG improved perturbation theory. E.g., the naive NLL result for  $\lambda(\mu)$ , (2.3), partially resums NNLL logarithms  $\lambda^{n+3}(\mu_0) \ln^n(\mu/\mu_0)$ . However, there are further NNLL terms from irreducible three-loop contributions. Therefore, the naive NLL result contains an inconsistent resummation of NNLL terms. Similarly, Eq. (2.4) includes an inconsistent resummation of higher-order terms, even though it is correct to the order considered. This fact is true whenever beta functions are integrated numerically at and beyond two loops.

For a *consistent* result, one needs to ignore terms of the neglected order in  $\lambda$  when integrating (2.1). This yields the consistent NNLL result

---

<sup>3</sup>Setting  $\beta_2 = 0$ , Eq. (2.4) reduces to (2.3), of course.

$$\frac{\lambda(\mu_0)}{\lambda(\mu)} = 1 - \beta_0 \hat{\lambda}(\mu_0) \ln\left(\frac{\mu}{\mu_0}\right) + \frac{\beta_1}{\beta_0} \hat{\lambda}(\mu_0) \ln\left(\frac{\lambda(\mu_0)}{\lambda(\mu)}\right) + \frac{\beta_1^2 - \beta_0 \beta_2}{\beta_0^2} \hat{\lambda}(\mu_0) \left[ \hat{\lambda}(\mu) - \hat{\lambda}(\mu_0) \right]. \quad (2.5)$$

The consistent NLL result is obtained from (2.5) by dropping the underlined terms. The final result for the consistent solution is obtained by solving Eq. (2.5) numerically.

Third we solve (2.5) iteratively by first substituting the one-loop result for  $\lambda(\mu)$  into the RHS of the equation above and then repeating this step with the result of the first substitution. This yields the *iterative* answer

$$\lambda(\mu) = \lambda(\mu_0) \left\{ 1 - \beta_0 \hat{\lambda}(\mu_0) \ln\left(\frac{\mu}{\mu_0}\right) + \frac{\beta_1}{\beta_0} \hat{\lambda}(\mu_0) \ln \left[ 1 - \beta_0 \hat{\lambda}(\mu_0) \ln \frac{\mu}{\mu_0} + \frac{\beta_1}{\beta_0} \hat{\lambda}(\mu_0) \ln \left( 1 - \beta_0 \hat{\lambda}(\mu_0) \ln \frac{\mu}{\mu_0} \right) \right] + \frac{\beta_1^2 - \beta_0 \beta_2}{\beta_0} \hat{\lambda}^3(\mu_0) \ln \frac{\mu}{\mu_0} \cdot \left( 1 - \beta_0 \hat{\lambda}(\mu_0) \ln \frac{\mu}{\mu_0} \right)^{-1} \right\}^{-1}. \quad (2.6)$$

We stress that no further expansions in  $\hat{\lambda}(\mu_0)$  are possible, because each  $\hat{\lambda}(\mu_0)$  multiplies a large logarithm  $\ln(\mu/\mu_0)$ . Eq. (2.6) is the NNLL result, and the NLL expression is again obtained by dropping the underlined terms.

The fourth solution of (2.1) is constructed in analogy to QCD: The integration constant obtained in the integration of (2.1) can be absorbed into a scale parameter  $\Lambda_H$ :

$$\frac{\lambda(\mu)}{16\pi^2} = \frac{2}{\beta_0 \ln(\frac{\Lambda_H^2}{\mu^2})} \left[ 1 - \frac{2\beta_1}{\beta_0^2} \frac{\ln[\ln(\frac{\Lambda_H^2}{\mu^2})]}{\ln(\frac{\Lambda_H^2}{\mu^2})} + \frac{4\beta_1^2}{\beta_0^4} \frac{\ln^2[\ln(\frac{\Lambda_H^2}{\mu^2})]}{\ln^2(\frac{\Lambda_H^2}{\mu^2})} - 4 \frac{\beta_1^2}{\beta_0^4} \frac{\ln[\ln(\frac{\Lambda_H^2}{\mu^2})]}{\ln^2(\frac{\Lambda_H^2}{\mu^2})} + 4 \frac{\beta_0 \beta_2 - \beta_1^2}{\beta_0^4} \frac{1}{\ln^2(\frac{\Lambda_H^2}{\mu^2})} + O\left(\frac{\ln^3[\ln(\frac{\Lambda_H^2}{\mu^2})]}{\ln^3(\frac{\Lambda_H^2}{\mu^2})}\right) \right]. \quad (2.7)$$

We call this result the *QCD-like* solution. The above equation defines the scale parameter  $\Lambda_H$ , and it is written such that no term of the form *const.* /  $\ln(\Lambda_H^2/\mu^2)$  appears in the square brackets. This is identical to the definition of the QCD scale parameter  $\Lambda_{\text{QCD}}^{\overline{\text{MS}}}$  [3]. The definition of the NLL parameter  $\Lambda_H^{\text{NLL}}$  is obtained by dropping the underlined terms. The above definition of  $\Lambda_H$  works in any renormalization scheme. The actual numerical evaluation of  $\Lambda_H$  depends on the boundary value  $\lambda(\mu_0)$ , which is scheme dependent. If for example  $\lambda(\mu)$  on the LHS of (2.7) is given in the  $\overline{\text{MS}}$ -scheme,  $\Lambda_H$  on the RHS equals  $\Lambda_H^{\overline{\text{MS}}}$ .

There are two important differences between the Higgs sector and QCD: First, Eq. (2.7) holds for  $\mu \ll \Lambda_H$ , while in an asymptotically free theory like QCD the analogue of (2.7) is valid for  $\mu \gg \Lambda_{\text{QCD}}$ . Second,  $\Lambda_{\text{QCD}}$  is the only fundamental scale parameter of QCD (with massless quarks), while in the Higgs sector  $\Lambda_H$  is related to the Higgs mass (see Table I). Yet if the Higgs mass turns out to be large, one will have to parametrize non-perturbative effects in terms of an

effective Lagrangian, and  $\Lambda_H$  will be the natural scale entering the effective couplings. In QCD perturbation theory breaks down for  $\mu \lesssim 3 \Lambda_{\text{QCD}}^{\overline{\text{MS}}}$  and binding energies equal a few times  $\Lambda_{\text{QCD}}$ . In the Higgs sector the breakdown of perturbation theory likewise occurs for  $\mu \gtrsim \Lambda_H/3$ . In Table I we tabulate the relation between  $M_H$  and  $\Lambda_H$ . When the OMS scheme is adopted,  $M_H$  in Table I is the physical mass (see (1.1)). In other schemes the tabulated values for  $M_H$  correspond to the tree-level relation  $\lambda(\mu_0 = M_H^{\text{tree}}) = (M_H^{\text{tree}})^2/(2v^2)$  and — in contrast to the OMS scheme — radiative corrections to this relation have to be taken into account in order to obtain the physical Higgs mass from  $M_H^{\text{tree}}$ . For the  $\overline{\text{MS}}$ -scheme this relation is encoded in (3.3) of Sect. III.

$M_H^{\text{tree}}(\text{GeV})$	$\Lambda_H^{\text{LL}}(\text{GeV})$	$\Lambda_H^{\text{NLL}}(\text{GeV})$	$\Lambda_{H,\text{OMS}}^{\text{NNLL}}(\text{GeV})$	$\Lambda_{H,\overline{\text{MS}}}^{\text{NNLL}}(\text{GeV})$	$\mu_{\text{max}}^{\text{NLL}}(\text{GeV})$
100.	$4 \cdot 10^{36}$	$6 \cdot 10^{37}$	$7 \cdot 10^{37}$	$7 \cdot 10^{37}$	$2.2 \cdot 10^{36}$
200.	$9 \cdot 10^{10}$	$6 \cdot 10^{11}$	$7 \cdot 10^{11}$	$7 \cdot 10^{11}$	$5.1 \cdot 10^{10}$
300.	$2.1 \cdot 10^6$	$8.7 \cdot 10^6$	$1.0 \cdot 10^7$	$1.0 \cdot 10^7$	$1.2 \cdot 10^6$
400.	$5.8 \cdot 10^4$	$1.8 \cdot 10^5$	$2.0 \cdot 10^5$	$2.1 \cdot 10^5$	$3.4 \cdot 10^4$
500.	$1.2 \cdot 10^4$	$2.9 \cdot 10^4$	$3.3 \cdot 10^4$	$3.6 \cdot 10^4$	$7.0 \cdot 10^3$
600.	$5.51 \cdot 10^3$	$1.13 \cdot 10^4$	$1.25 \cdot 10^4$	$1.40 \cdot 10^4$	$3.2 \cdot 10^3$
700.	$3.57 \cdot 10^3$	$6.45 \cdot 10^3$	$6.92 \cdot 10^3$	$7.99 \cdot 10^3$	$2.1 \cdot 10^3$
800.	$2.78 \cdot 10^3$	$4.52 \cdot 10^3$	$4.71 \cdot 10^3$	$5.64 \cdot 10^3$	$1.6 \cdot 10^3$
900.	$2.41 \cdot 10^3$	$3.57 \cdot 10^3$	$3.60 \cdot 10^3$	$4.52 \cdot 10^3$	$1.40 \cdot 10^3$
1000.	$2.22 \cdot 10^3$	$3.03 \cdot 10^3$	$2.94 \cdot 10^3$	$3.91 \cdot 10^3$	$1.29 \cdot 10^3$
1100.	$2.13 \cdot 10^3$	$2.68 \cdot 10^3$	$2.48 \cdot 10^3$	$3.57 \cdot 10^3$	$1.24 \cdot 10^3$
1200.	$2.09 \cdot 10^3$	$2.41 \cdot 10^3$	$2.18 \cdot 10^3$	$3.37 \cdot 10^3$	$1.21 \cdot 10^3$

TABLE I. The values for the scale parameter  $\Lambda_H$  obtained from (2.7) for  $\mu_0 = M_H^{\text{tree}}$ .  $M_H^{\text{tree}}$  in the left column corresponds to  $M_H^{\text{tree}} = v\sqrt{2\lambda(\mu_0 = M_H^{\text{tree}})}$ . For  $\lambda = \lambda_{\text{OMS}}$  this relation receives no radiative corrections. If the coupling is defined in the  $\overline{\text{MS}}$ -scheme, use (3.4) first to calculate  $\lambda_{\overline{\text{MS}}}(\mu_0 = M_H^{\text{tree}})$  from the physical Higgs mass to the desired order. Then use the previous equation to obtain  $M_H^{\text{tree}}$ .  $\Lambda_H^{\text{LL}}$  corresponds to the location of the one-loop Landau pole. The difference between the fourth and fifth column is caused by the scheme dependence of  $\beta_2$ . The last column contains the two-loop values of  $\mu$  for which the iterative solution, (2.6), assumes its maximum.

We now completed the definition of the four different solutions for the running Higgs coupling: naive, consistent, iterative, and QCD-like solution. It is interesting to note that at one loop all four solutions are identical.<sup>4</sup> This is clearly not the case anymore at two-loop and higher orders, and we will discuss the differences below. Let us stress again that *all* solutions correctly sum the large logarithm  $\ln(\mu/\mu_0)$  within the calculated order. The difference between these solutions is of the neglected order as can be seen when expanding the solutions in  $\lambda(\mu_0)$ . If perturbation theory is applicable this difference should be numerically small, giving a very simple criterion to find the values of  $M_H$  and  $\mu$  beyond which perturbation theory clearly fails.

In Fig. 1, we compare the  $\mu$  dependence of the four solutions at one and two loops. We choose the three mass values  $M_H = 200, 500, \text{ and } 800 \text{ GeV}$ . To obtain a meaningful compari-

<sup>4</sup>To see this, set  $\beta_1 = \beta_2 = 0$  in the four different solutions.

son between the one- and two-loop results for a given value of  $M_H$ , we take for both orders the same expansion parameter  $\lambda_0 \equiv \lambda(\mu_0)$ , and choose it to be defined by the tree-level relationship  $\lambda_0 = (M_H^{\text{tree}})^2/(2v^2)$ . This has the additional advantage that we do not yet have to specify a renormalization scheme in Fig. 1. Since the first two coefficients of the  $\beta$ -function are scheme independent, the whole scheme dependence resides in the relation between the tree-level mass (which labels the different curves in Fig. 1) and the physical Higgs mass. In the OMS, the two mass definitions coincide.

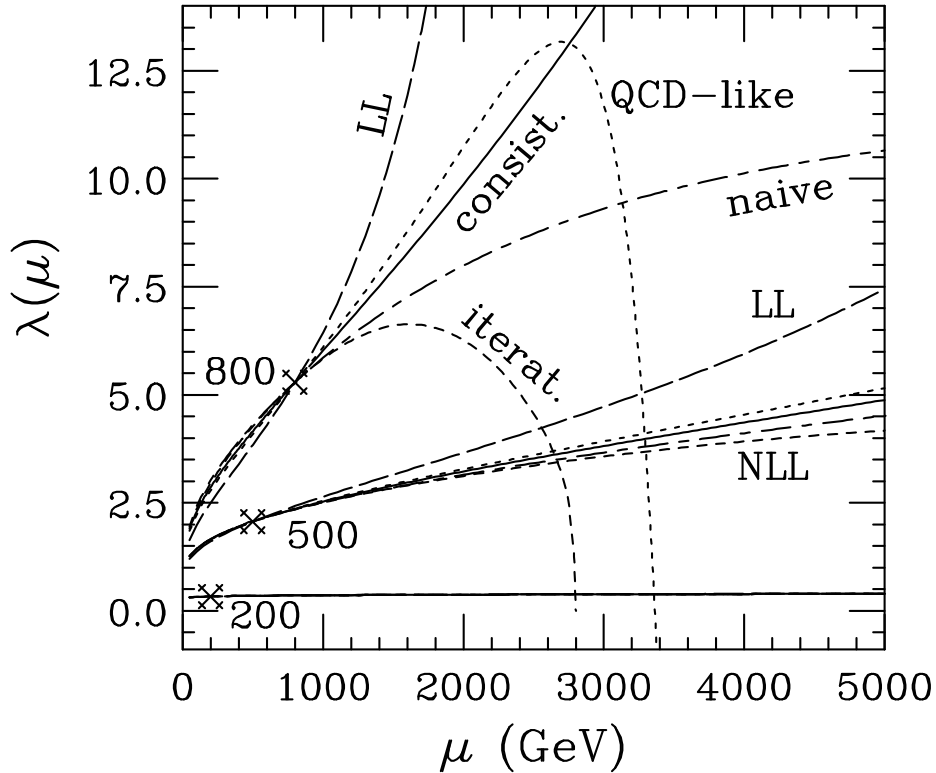


FIG. 1. Different solutions of the one-loop and two-loop RGE equations for the Higgs quartic coupling  $\lambda$ : the one-loop solution (long dashes), the two-loop naive solution according to (2.3) (long-short dashes), the two-loop consistent solution of (2.5) (solid line), the two-loop iterative solution (2.6) (short dashes), and the two-loop QCD-like solution expanded in powers of  $1/\ln(\Lambda_H^2/\mu^2)$  given in (2.7) (dots). The crosses show the normalization point:  $\lambda(\mu = M_H^{\text{tree}}) = \lambda_0$ . To allow for a meaningful comparison of the different orders in perturbation theory, we choose  $\lambda_0$  to be the same at one and two loops. The curves are labeled by the tree-level Higgs mass (in GeV), corresponding to the tree level relation  $\lambda_0 = (M_H^{\text{tree}})^2/(2v^2)$ . In renormalization schemes different from the OMS, radiative corrections to this relation must be included (see text).

At one loop, the four solutions are identical (long dashed curve). The coupling  $\lambda^{\text{LL}}(\mu)$  approaches infinity as  $\mu \rightarrow \Lambda_H^{\text{LL}}$ , which is usually referred to as the Landau pole [4]. At two loops the breakdown of perturbation theory is clearly visible in the two-loop curves for  $M_H = 800$  GeV. It manifests itself in a very different behaviour of the four solutions, although they all are defined to have the same value for  $\mu_0 = M_H$ . The one-loop Landau pole has completely vanished from all two-loop solutions. The naive (long-short dashes in Fig. 1) and consistent (solid) solutions always

have positive slopes in accordance with the positiveness of the perturbative  $\beta$ -function, Eq. (2.1). The consistent solution can be looked at as the “average” of the one-loop solution and the two-loop naive solution. The naive solution approaches the fix-point value  $\lambda_{\max}^{\text{NLL}} = 12.147$ , the zero of the two-loop beta function. This simply reflects the fact that one cannot use perturbation theory to gain information about large values of the coupling. This is even more evident from the other two solutions. The QCD-like result for  $\lambda^{\text{NLL}}(\mu)$  has a global maximum. Interestingly enough, for values of  $M_H > 1263$  GeV, the value  $\lambda_0 = M_H^2/(2v^2)$  is larger than the maximal possible value of the QCD-like running coupling, so that  $\lambda(\mu = M_H) = \lambda_0$  can no longer be satisfied. The unphysical maximum of the QCD-like solution appears for  $\mu_{\max}^{\text{QCD}} = \Lambda_H^{\text{NLL}}/1.7$ , and perturbation breaks down well before  $\mu$  is equal to  $\Lambda_H$ . The iterative solution features a maximum at

$$\mu_{\max}^{\text{iter}} = M_H \exp \left( \frac{1 + \frac{\beta_1}{\beta_0} \hat{\lambda}_0}{\beta_0 \hat{\lambda}_0} \right) = 0.58 M_H \exp \left( \frac{6.58}{\lambda(\mu_0)} \right), \quad (2.8)$$

which is located at 1615 (7033) GeV for  $M_H = 800$  (500) GeV. The two-loop iterative solution approaches zero at the same value of  $\mu$  at which the one-loop solution has its Landau pole.

The fact that some perturbative solutions of the two-loop running coupling show a maximum gives a first criterion for the breakdown of the two-loop perturbative treatment. From the definition of the  $\beta$  function, Eq. (2.1), we know that in the perturbative regime the slope of the running coupling has to be positive as the one-loop term dominates over the two-loop term. If the iterative solution for  $\lambda(\mu)$  has negative slope, then perturbation theory is not valid anymore. Hence Eq. (2.8) is possibly a measure of the range of  $\mu$  for which perturbation theory is meaningful.

The previous discussion of the four solutions is valid for any value of  $M_H$ . Yet if we restrict ourselves to values  $\mu < 5000$  GeV, features like poles and maxima are only apparent for  $M_H = 800$  GeV, and not for 500 and 200 GeV (see Fig. 1). For the lower mass values one has to go to (much) larger values of  $\mu$  to observe the breakdown of perturbation theory. In fact, if  $M_H = 200$  GeV all four solutions of the running coupling agree extremely well for  $\mu < 5000$  GeV. Choosing  $M_H = 500$ , however, already results in an uncertainty between the different two-loop solutions of about 25% at  $\mu = 5$  TeV, and the one-loop solution is more than 50% larger than the two-loop solution at  $\mu = 5$  TeV.

If the Standard Model Higgs sector is to remain perturbative up to much higher energy scales the restrictions on  $M_H$  get much more severe [5]. To avoid the Landau pole and keeping the coupling  $\lambda$  perturbative, one can define an embedding scale below the Landau pole and require the running coupling to be smaller than a certain value. For example, taking the embedding scale to be  $10^{10}$  GeV the authors of [6] implement the “automatic fixing procedure” requiring (in our notation)  $\lambda(10^{10}\text{GeV}) < \pi^2$  and find an upper bound of  $M_H \approx 230$  GeV when neglecting the top-quark Yukawa coupling. Using Eq. (2.8) and requiring  $\mu_{\max}^{\text{iter}}$  to be equal or larger than  $10^{10}$  GeV, we find the upper limit  $M_H \approx 210$  GeV.

The analysis of the running coupling alone can clearly only yield a necessary criterion for the validity of perturbation theory. Taking  $M_H = 800$  GeV, we can be sure that perturbation theory breaks down for any cross section with  $\sqrt{s} \approx 2$  TeV, because this energy is too close [7] to the scale parameter  $\Lambda_H$  and already larger than the corresponding maximum of  $\mu$ ,  $\mu_{\max}^{\text{iter}}(M_H = 800\text{GeV}) \approx 1600$  GeV. For  $M_H \leq 500$  GeV, the perturbative RG treatment of the running coupling could be trustworthy up to values of  $\mu_{\max}^{\text{iter}} \approx 7$  TeV, sufficient for studying Higgs physics at the LHC. Nevertheless, choosing  $M_H = 500$  GeV the running coupling  $\lambda^{\text{NLL}}(\mu = 7\text{TeV}) = 4.4$  is sizable.



To make a final judgement on whether perturbation theory works for  $M_H = 500$  GeV and TeV-energies, one must in addition investigate the perturbation series of the physical process of interest. As we will see later on, the perturbative solution of the running coupling may show a reasonable convergence, but the numerical value of the running coupling is already too large to calculate physical quantities like cross sections and decay widths in perturbation theory. This will be the subject of sections IV and V.

### III. SCHEME DEPENDENCE: OMS VS. $\overline{\text{MS}}$ FORMULATION

So far the discussion of the running coupling has been independent of a special renormalization scheme. We have already listed the reasons for studying different renormalization schemes in the introduction.

In the following we will look at the  $\overline{\text{MS}}$  and OMS scheme, and examine the scheme dependence of the coupling and the three-loop coefficient  $\beta_2$  in (2.1). Before going into detail we would like to remark two points: First, the OMS coupling  $\lambda_{\text{OMS}}$  is to all orders in  $\lambda$  directly related to measurable quantities (the muon lifetime and the Higgs mass) via (1.1). This is not so for any other renormalization scheme, where the RHS of (1.1) receives radiative corrections, which depend on an additional parameter, the *renormalization point*  $\mu_0$ . Second the scheme dependence of  $\beta_2$  makes the coupling run differently in different schemes. One can in general adjust the scheme such as to achieve any desired values for  $\beta_n$  with  $n \geq 2$ . A criterion for a “good scheme”, however, cannot be founded on the smallness of the running coupling alone. Instead one has to consider physical observables, in which the coefficients of the perturbation series depend on the scheme as well. This will be done in the following sections.

The starting point of the analysis is the two-loop relation between the bare and the renormalized coupling:

$$\begin{aligned} \mu^{-2\epsilon} \hat{\lambda}^{\text{bare}} = & \hat{\lambda} + \hat{\lambda}^2 \xi^\epsilon \left[ \frac{\beta_0}{2} \frac{1}{\epsilon} + c_1 + \epsilon c_{11} + \epsilon^2 c_{12} + O(\epsilon^3) \right] \\ & + \hat{\lambda}^3 \xi^{2\epsilon} \left[ \frac{\beta_0^2}{4} \frac{1}{\epsilon^2} + \left( \beta_0 c_1 + \frac{\beta_1}{4} \right) \frac{1}{\epsilon} + c_2 + \epsilon c_{21} + O(\epsilon^2) \right] \\ & + \hat{\lambda}^4 \xi^{3\epsilon} \left[ \frac{\beta_0^3}{8} \frac{1}{\epsilon^3} + \left( \frac{3}{4} \beta_0^2 c_1 + \frac{7}{24} \beta_0 \beta_1 \right) \frac{1}{\epsilon^2} \right. \\ & \quad \left. + \left( -\frac{5}{12} \beta_0^2 c_{11} + \frac{1}{3} \beta_0 c_1^2 + \frac{7}{6} \beta_0 c_2 + \frac{7}{12} \beta_1 c_1 + \frac{1}{6} \beta_2 \right) \frac{1}{\epsilon} + c_3 + O(\epsilon) \right]. \quad (3.1) \end{aligned}$$

In the  $\overline{\text{MS}}$ -scheme the various quantities are given as

$$\hat{\lambda} = \frac{\lambda_{\overline{\text{MS}}}(\mu)}{16\pi^2}, \quad \xi = 4\pi e^{-\gamma_E}, \quad c_1 = c_2 = c_3 = c_{11} = c_{12} = c_{21} = 0.$$

In the OMS scheme, they instead read [8,9]:

$$\hat{\lambda} = \frac{\lambda_{\text{OMS}}}{16\pi^2}, \quad \xi = \frac{4\pi\mu^2 e^{-\gamma_E}}{M_H^2}, \quad c_1 = 25 - 3\pi\sqrt{3} = 8.676, \quad c_2 = 378.5, \quad c_{11} = 3.821, \quad (3.2)$$

and  $c_3$ ,  $c_{12}$ , and  $c_{21}$  are unknown. Knowing the bare coupling to two loops in both the OMS scheme and the  $\overline{\text{MS}}$  scheme, we can express the  $\overline{\text{MS}}$  coupling in terms of the OMS coupling, and we can calculate the difference between  $\beta_2^{\text{OMS}}$  and  $\beta_2^{\overline{\text{MS}}}$ .

### A. The $\overline{\text{MS}}$ -coupling $\lambda_{\overline{\text{MS}}}$ and the renormalization point $\mu_0$

Since the OMS coupling is a function of  $M_H$  (or  $v$ ) and is fixed to all orders by (1.1), the definition of  $\lambda_{\overline{\text{MS}}}$  in terms of  $\lambda_{\text{OMS}}$  is equivalent to a relation between  $\lambda_{\overline{\text{MS}}}$  and  $M_H$ . With  $c_i$  and  $c_{ij}$  referring to the OMS quantities in (3.2) we find:

$$\begin{aligned} \lambda_{\overline{\text{MS}}}(\mu_0) = \lambda_{\text{OMS}} & \left[ 1 + \left( \frac{\beta_0}{2} \ln \frac{\mu_0^2}{M_H^2} + c_1 \right) \hat{\lambda}_{\text{OMS}} \right. \\ & + \left( \left( \frac{\beta_0}{2} \right)^2 \ln^2 \frac{\mu_0^2}{M_H^2} + \left( \frac{\beta_1}{2} + \beta_0 c_1 \right) \ln \frac{\mu_0^2}{M_H^2} + c_2 - \beta_0 c_{11} \right) \hat{\lambda}_{\text{OMS}}^2 \\ & + \left( \left( \frac{\beta_0}{2} \right)^3 \ln^3 \frac{\mu_0^2}{M_H^2} + \frac{\beta_0}{2} \left( \frac{5}{4} \beta_1 + \frac{3}{2} \beta_0 c_1 \right) \ln^2 \frac{\mu_0^2}{M_H^2} \right. \\ & \quad \left. + \left( (3c_2 - 3\beta_0 c_{11}) \frac{\beta_0}{2} + \beta_1 c_1 + \frac{1}{2} \beta_2^{\text{OMS}} \right) \ln \frac{\mu_0^2}{M_H^2} \right. \\ & \quad \left. + c_3 + \left( \frac{1}{4} \beta_0 c_{12} - c_1 c_{11} - c_{21} \right) \beta_0 - \frac{3}{4} \beta_1 c_{11} \right) \hat{\lambda}_{\text{OMS}}^3 \\ & \left. + \mathcal{O}(\hat{\lambda}_{\text{OMS}}^4) + \mathcal{O}(\epsilon) \right], \end{aligned} \quad (3.3)$$

$$\begin{aligned} = \hat{\lambda}_{\text{OMS}} & \left[ 1 + \left( 12 \ln \frac{\mu_0^2}{M_H^2} + 8.676 \right) \hat{\lambda}_{\text{OMS}} \right. \\ & + \left( 144 \ln^2 \frac{\mu_0^2}{M_H^2} + 52.22 \ln \frac{\mu_0^2}{M_H^2} + 286.8 \right) \hat{\lambda}_{\text{OMS}}^2 \\ & + \left( 1728 \ln^3 \frac{\mu_0^2}{M_H^2} - 932.0 \ln^2 \frac{\mu_0^2}{M_H^2} + 9736.8 \ln \frac{\mu_0^2}{M_H^2} + d_{30} \right) \hat{\lambda}_{\text{OMS}}^3 \\ & \left. + \mathcal{O}(\epsilon) \right], \end{aligned} \quad (3.4)$$

which agrees to one loop with the result of Sirlin and Zucchini [10]. The three-loop constant term  $d_{30}$  depends on the yet unknown OMS coefficients  $c_{12}$ ,  $c_{21}$ , and  $c_3$ .

For convenience we give the inverse formula of (3.4) as well:

$$\begin{aligned} \lambda_{\text{OMS}} = \lambda_{\overline{\text{MS}}}(\mu) & \left[ 1 + \left( -12 \ln \frac{\mu^2}{M_H^2} - 8.676 \right) \hat{\lambda}_{\overline{\text{MS}}}(\mu) \right. \\ & + \left( 144 \ln^2 \frac{\mu^2}{M_H^2} + 364.2 \ln \frac{\mu^2}{M_H^2} - 136.3 \right) \hat{\lambda}_{\overline{\text{MS}}}^2(\mu) \\ & \left. + \mathcal{O}(\hat{\lambda}_{\overline{\text{MS}}}^3) + \mathcal{O}(\epsilon) \right]. \end{aligned} \quad (3.5)$$

Eq. (3.3) defines the expansion parameter  $\lambda(\mu_0)$  of the running coupling when using the  $\overline{\text{MS}}$  scheme. It shows that  $\lambda_{\overline{\text{MS}}}$  is completely determined by specifying  $M_H$  (and thereby  $\lambda_{\text{OMS}}$ ) and a renormalization point  $\mu_0$  at which (3.3) is imposed. The scale  $\mu_0$  is unspecified. However, to ensure that the logarithms  $\ln(\mu_0/M_H)$  stay small at all orders, it should be chosen of the order of  $M_H$ .

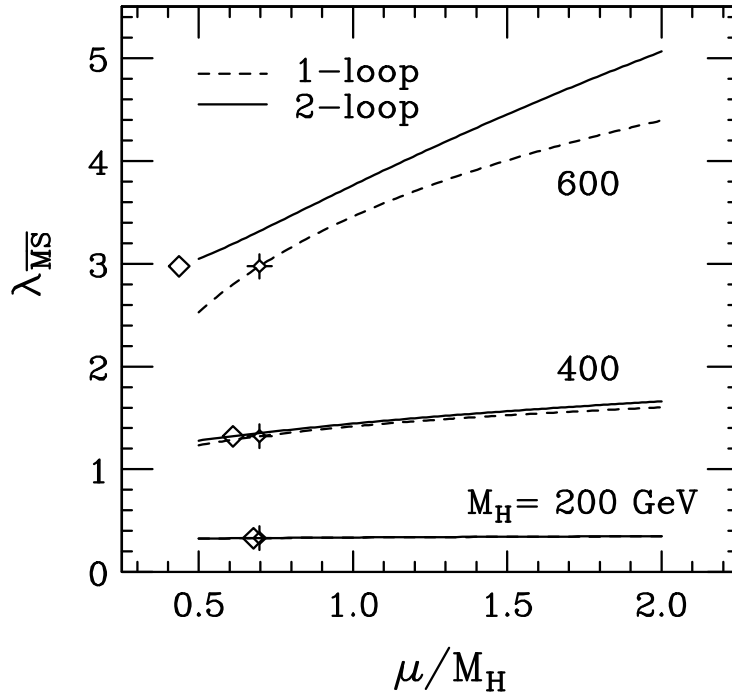


FIG. 2. The  $\overline{\text{MS}}$  coupling,  $\lambda_{\overline{\text{MS}}}$ , as a function of the renormalization scale  $\mu$ , fixing the physical Higgs mass at 200, 400, and 600 GeV. The value of  $\mu$  at which the two-loop (one-loop)  $\overline{\text{MS}}$  coupling is equal to the  $\mu$ -independent OMS-coupling,  $\lambda_{\text{OMS}}$ , is indicated by a diamond (crossed diamond).

Let us emphasize that throughout the paper  $M_H$  denotes the pole mass, even when discussing  $\overline{\text{MS}}$  renormalization, and the vacuum expectation value  $v$  is also chosen as defined in the OMS as in [10]. Expressions involving the running mass of the  $\overline{\text{MS}}$ -scheme can systematically be expressed in terms of the pole mass  $M_H$ . Despite the use of the pole mass  $M_H$ , the  $\overline{\text{MS}}$  renormalization scheme maintains all the advantages of mass independent schemes mentioned in the introduction. For example  $\lambda_{\overline{\text{MS}}}(\mu_0 = M_H) = (800 \text{ GeV})^2/(2v^2)$  corresponds to a physical Higgs mass of  $M_H = 720 \text{ GeV}$  at one loop, and  $M_H = 681 \text{ GeV}$  at two loops.

In Fig. 2 we show the  $\overline{\text{MS}}$  coupling as a function of  $\mu_0$  for different values of  $M_H$ , varying  $\mu_0$  in a typical range,  $M_H/2 \leq \mu_0 \leq 2M_H$ . We find that the  $\overline{\text{MS}}$  coupling is larger than the OMS coupling for most of the range of  $\mu_0$  examined. If  $M_H$  is larger than 400 GeV, the value of  $\mu_0$  at which  $\lambda_{\overline{\text{MS}}}(\mu_0)$  equals  $\lambda_{\text{OMS}}$  changes significantly when going from one loop to two loops. At one loop, the two couplings are equal if  $\mu_0 \approx 0.7 M_H$  for any value of  $M_H$ , because  $\beta_0/2 \cdot \ln(0.7^2) = -c_1$ . At two loops, the relation gets a more complicated mass dependence. We find that for  $M_H = 400$  (600) GeV the two-loop couplings of the two schemes are equal if  $\mu_0 = 0.6 M_H$  ( $0.4 M_H$ ).

At first sight it appears reasonable to choose  $\mu_0$  in such a way that calculated radiative corrections become small or even zero. This criterion of (*fastest*) *apparent convergence* (FAC) has had some supporters in QCD RG analyses over a decade ago (for a criticism see [11]). Also in [10] the one-loop FAC scale  $\mu_0 = 0.7 M_H$ , at which the one-loop correction in (3.3) vanishes, has been used to define  $\lambda_{\overline{\text{MS}}}$ . Yet in the following we will explain why this choice of the scale is not very

useful, in particular in conjunction with the analysis of the breakdown of perturbation theory. We can already anticipate this fact from the above observation that for large values of  $M_H$  the two-loop FAC scale differs sizably from its one-loop value. For a more detailed investigation consider the generalization of the square bracket in (3.3) to the order  $\hat{\lambda}_{\text{OMS}}^N$ :

$$\hat{\lambda}_{\overline{\text{MS}}}(\mu_0) = \hat{\lambda}_{\text{OMS}} \left[ 1 + \sum_{n=1}^N \hat{\lambda}_{\text{OMS}}^n \sum_{k=0}^n d_{nk} \ln^k \frac{\mu_0^2}{M_H^2} \right], \quad (3.6)$$

i.e. one has  $d_{10} = c_1$ ,  $d_{11} = \beta_0/2$  and so on. Application of the renormalization group equation (2.1) (with  $\mu = \mu_0$ ) yields recursion relations for the  $d_{nk}$ 's. The solution for the coefficients  $d_{nn}$  of the leading logarithms is well-known:

$$d_{nn} = \left( \frac{\beta_0}{2} \right)^n. \quad (3.7)$$

Similarly we derive the general relationship

$$d_{n,n-1} = c_1 n \left( \frac{\beta_0}{2} \right)^{n-1} + a_n \frac{\beta_1}{2} \left( \frac{\beta_0}{2} \right)^{n-2} \quad (3.8)$$

for the next-to-leading logarithms with

$$a_n = \sum_{k=1}^{n-1} \sum_{j=1}^k \frac{1}{j} = n [\psi(n+1) + \gamma_E - 1],$$

where  $\psi(x) = \frac{d}{dx} \ln \Gamma(x)$ . For  $n \leq 3$  the coefficients  $d_{nn}$  and  $d_{n,n-1}$  have already been given in (3.3), where also the NNLL coefficient  $d_{31}$  involving  $\beta_2$  is displayed.

We remark here that the coefficients (3.7) and (3.8) have the same form for any expansion of a running coupling  $\lambda(\mu)$  in terms of some  $\mu$ -independent coupling with only the coefficient  $c_1$  changed correspondingly. For example, the expansion of  $\lambda_{\overline{\text{MS}}}(\mu)$  in terms of  $\lambda_{\overline{\text{MS}}}(M_H)$  yields a series of the form (3.6) with  $\hat{\lambda}_{\text{OMS}} \rightarrow \hat{\lambda}_{\overline{\text{MS}}}(M_H)$  and  $d_{10} = c_1 \rightarrow 0$  in (3.8).

Now the choice  $\mu_0 = M_H$  nullifies all logarithms to all orders in (3.6). The FAC scale  $\mu_0 = 0.7 M_H$  instead nullifies the  $\hat{\lambda}_{\text{OMS}}^1$ -term in (3.6) and (3.3), but the price to be paid is the appearance of logarithms in higher orders. Since we know the NLL coefficients  $c_2$  and  $c_{11}$ , we can check the effect of the FAC scale setting on the  $\hat{\lambda}_{\text{OMS}}^2$ -term in (3.3): For  $\mu_0 = M_H$  the coefficient of  $\hat{\lambda}_{\text{OMS}}^2$  equals 287, but for  $\mu_0 = 0.7 M_H$  one finds the larger coefficient 324 which increases the impact of higher order terms, especially if the coupling is large. This explains the above finding that the FAC scale changes significantly for large values of  $M_H$  when passing from the one-loop to the two-loop order. Hence the FAC scale setting pushes large terms from the calculated orders into the uncalculated higher orders of the perturbation series. Yet a clever choice of  $\mu_0$  should yield the opposite and keep these higher order terms small.

Of course one is not forced to use  $\mu_0 = M_H$  exactly. But what is the allowed range for  $\mu_0$ ? Clearly  $\ln(\mu_0^2/M_H^2)$  in (3.6) must be kept small, so that the logarithms do not become dominant in higher orders. A reasonable interval for  $\mu_0$  should therefore obey

$$\left| d_{n,m+1} \ln^{m+1} \frac{\mu_0^2}{M_H^2} \right| \lesssim \left| d_{nm} \ln^m \frac{\mu_0^2}{M_H^2} \right|$$

for  $m = 0, \dots, n-1$ . Especially the size of the logarithms should not exceed the constant term  $|d_{n0}|$ . With the two-loop information (3.4) at hand we first compare the size of both  $d_{22} \ln^2(\mu_0^2/M_H^2)$  and  $d_{21} \ln(\mu_0^2/M_H^2)$  with the non-logarithmic term,  $d_{20} = 286.8$ , and find that for  $0.5 \leq \mu_0/M_H \leq 2.0$  their magnitudes do not exceed  $|d_{20}|$ . Second, using (3.7) and (3.8) we can compare the leading logarithm  $d_{nn} \ln^n(\mu_0^2/M_H^2)$  with the next-to-leading logarithms  $d_{n,n-1} \ln^{n-1}(\mu_0^2/M_H^2)$  to all orders in perturbation theory obtaining the smaller range  $0.8 \leq \mu_0/M_H \leq 1.25$ . At three loops we can use the result (3.11) to repeat the game with the next-to-next-to-leading logarithm, which is multiplied by  $d_{31} = 9736.8$  in (3.3):  $|d_{33} \ln^3(\mu_0^2/M_H^2)|$  and  $|d_{32} \ln^2(\mu_0^2/M_H^2)|$  are smaller than  $|d_{31} \ln(\mu_0^2/M_H^2)|$  for  $0.3 \leq \mu_0/M_H \leq 3.3$ . For  $\mu_0/M_H = 0.3$  or  $\mu_0/M_H = 3.3$  this term, however, exceeds  $2 \cdot 10^4$ , which is above the value one expects for the yet unknown constant  $|d_{30}|$ . Since  $d_{33}, d_{31} > 0$  and  $d_{32} < 0$  the choice  $\mu_0/M_H = 0.7 < 1$ , which has been so seductive in the order  $\hat{\lambda}_{\text{OMS}}^1$ , leads to the fact that the three logarithmic terms in the order  $\hat{\lambda}_{\text{OMS}}^3$  add with the same sign to yield  $-8045$ . Moreover from (3.7) and (3.8) one realizes that for  $\mu_0 < M_H$  the leading and next-to-leading logarithmic terms have the same sign to all orders  $\hat{\lambda}_{\text{OMS}}^n$  except for  $n = 1$  and  $n = 2$ ! Hence the one-loop FAC choice  $\mu_0 = 0.7M_H$  pushes large terms into the higher orders. The two-loop FAC scale is even lower, increasing all higher order terms even more.

We conclude that our lack of knowledge of the higher order terms of the perturbation series forces us to consider *any* choice for  $\mu_0$  in the range  $0.8 \leq \mu_0/M_H \leq 1.25$  (which may possibly be relaxed to  $0.5 \leq \mu_0/M_H \leq 2.0$ ) with equal right. Changing  $\mu_0$  in the  $n$ -th order perturbative expression for some observable changes the result by terms of the neglected order  $\lambda^{n+1}$ . When perturbation theory works the dependence on  $\mu_0$  diminishes order-by-order in  $\lambda$ . We will use a similar criterion to find the breakdown of perturbation theory in sections IV and V.

Let us close this section with a final remark on the arbitrariness of  $\mu_0$ : Cross sections with cm-energy  $\sqrt{s}$  and expressed in terms of  $\lambda_{\overline{\text{MS}}}(\mu)$  involve the logarithm  $\ln(\mu^2/s)$ . Using (3.3) with  $\mu = \mu_0$ , this logarithm would be large. Using the running coupling  $\lambda_{\overline{\text{MS}}}(\mu)$  evaluated at a scale  $\mu \approx \sqrt{s}$ , the logarithm is summed to all orders in perturbation theory. The arbitrariness in the choice of  $\mu_0 \approx M_H$  and  $\mu \approx \sqrt{s}$  reflects the fact that one can sum an arbitrary small constant together with the large logarithm. This feature is also present in the OMS scheme, but less apparent. For example, the authors of [2] sum the constant  $c_1$  in (3.3) together with  $\ln(\mu^2/s)$ .

## B. The NNLL $\beta$ -function in the OMS and $\overline{\text{MS}}$ -scheme

Neglecting all couplings except for the Higgs coupling  $\lambda$ , the Higgs sector of the Standard Model is equivalent to a spontaneously broken  $\phi^4$  theory with  $N = 4$  real scalar fields. Theories with spontaneous symmetry breaking have the remarkable property that the counterterms needed to make the theory finite are the same for the broken and unbroken symmetry, if a mass independent renormalization scheme is adopted [12]. Since the beta coefficients are calculated from the counterterms of the coupling, Eq. (3.1), the beta function is also identical for both the broken and the unbroken theory. Hence one can calculate the  $(n+1)$ -loop coefficient  $\beta_n^{\text{OMS}}$  of the Higgs sector in two steps: First, obtain  $\beta_n^{\overline{\text{MS}}}$  in an unbroken  $\phi^4$  theory with  $N = 4$  real scalar fields by calculating the divergent parts of the four-point function to the  $(n+1)$ -loop order. This is easier than working in the broken theory, because only a four-point coupling is involved. Once this is accomplished,  $\beta_n^{\overline{\text{MS}}}$  of the broken theory is known, too. Second, calculate the scheme dependence  $\beta_n^{\overline{\text{MS}}} - \beta_n^{\text{OMS}}$ . This only requires the calculation of the  $n$ -loop (not  $n+1$ -loop) finite parts of self-energy diagrams.

The three-loop coefficient  $\beta_2$  of the  $\phi^4$  theory has been calculated in the  $\overline{\text{MS}}$  scheme [13]:

$$\beta_2^{\overline{\text{MS}}} = 7176 + 4032\zeta(3) = 12022.69 \dots \quad (3.9)$$

To obtain  $\beta_2^{\text{OMS}}$ , we return to Eq. (3.1) to calculate the scheme dependence of the coefficient  $\beta_2$ . As stated above, unlike  $\beta_2$  itself the scheme dependent difference between  $\beta_2^{\overline{\text{MS}}}$  and  $\beta_2^{\text{OMS}}$  can entirely be obtained from two-loop quantities:

$$\begin{aligned} \beta_2^{\overline{\text{MS}}} &= \beta_2^{\text{OMS}} - \beta_1 c_1 + \beta_0 c_2 - \beta_0 c_1^2 - \beta_0^2 c_{11} \\ &= \beta_2^{\text{OMS}} - 5400 + 8688\zeta(2) - 2160\zeta(3) - 2736\pi\sqrt{3} \\ &\quad + 1152\pi\text{Cl}(\pi/3) + 5184\sqrt{3}\text{Cl}(\pi/3) + 3888K_5 \\ &= \beta_2^{\text{OMS}} + 7784.45 \dots \end{aligned} \quad (3.10)$$

where  $K_5 = 0.92363 \dots$  is the value of the all massive Master diagram with  $p^2 = M_H^2$ , which has been evaluated numerically in [8]. (3.10) can be obtained from the definition (2.1) of the  $\beta$ -function or by comparing the bare coupling expressed in terms of  $\lambda_{\overline{\text{MS}}}$  with its expression in terms of  $\lambda_{\text{OMS}}$ .

Using the result for  $\beta_2^{\overline{\text{MS}}}$  we obtain

$$\beta_2^{\text{OMS}} = 4238.23 \dots \quad (3.11)$$

Our analytical<sup>5</sup> result agrees with the numerical result obtained in [14] to better than six digits.

In Fig. 3 we show the  $\mu$ -dependence of the NNLL (three-loop) running coupling in the OMS scheme. The consistent solution is almost identical to its NLL (two-loop) result even for  $M_H = 800$  GeV, whereas the other NNLL solutions show a behaviour very different from their NLL results for large  $M_H$ . For  $M_H = 500$  GeV and  $\mu < 5$  TeV all four NNLL solutions show a very nice convergence. For such a value of  $M_H$ , however, the LL running coupling is not an adequate approximation for the upper values of  $\mu$  considered.

In the  $\overline{\text{MS}}$  scheme, the convergence of the running coupling is rather poor for  $M_H = 500$  GeV and above. This is also true for the consistent solution. For  $M_H = 750$  GeV, the consistent NNLL solution of the  $\overline{\text{MS}}$  running coupling is not defined anymore if  $\mu > 950$  GeV. The poor performance of the NNLL  $\overline{\text{MS}}$  coupling is due to the term involving  $\beta_2$ . Although  $\beta_2^{\overline{\text{MS}}}$  is only three times larger than  $\beta_2^{\text{OMS}}$  the coefficient  $\beta_1^2 - \beta_0\beta_2$  entering the running coupling (2.5-2.7) is 44 times larger in the  $\overline{\text{MS}}$  scheme. This is caused by a numerical cancellation in the OMS scheme, where  $\beta_2^{\text{OMS}}/\beta_1 \approx \beta_1/\beta_0$ . We remark here that in a scheme with exact geometrical growth of the coefficients,  $\beta_{n+1}/\beta_n = \beta_1/\beta_0$ , the consistent solution (2.5) equals the consistent NLL result to all orders.

#### IV. SCHEME AND SCALE DEPENDENCE OF HIGGS DECAYS

The accuracy of perturbation theory and its breakdown as  $M_H$  increases can only be investigated in physical observables. Here processes in which all mass parameters are of the order of

---

<sup>5</sup>apart from the numerical constant  $K_5$  which is defined by a single Feynman diagram

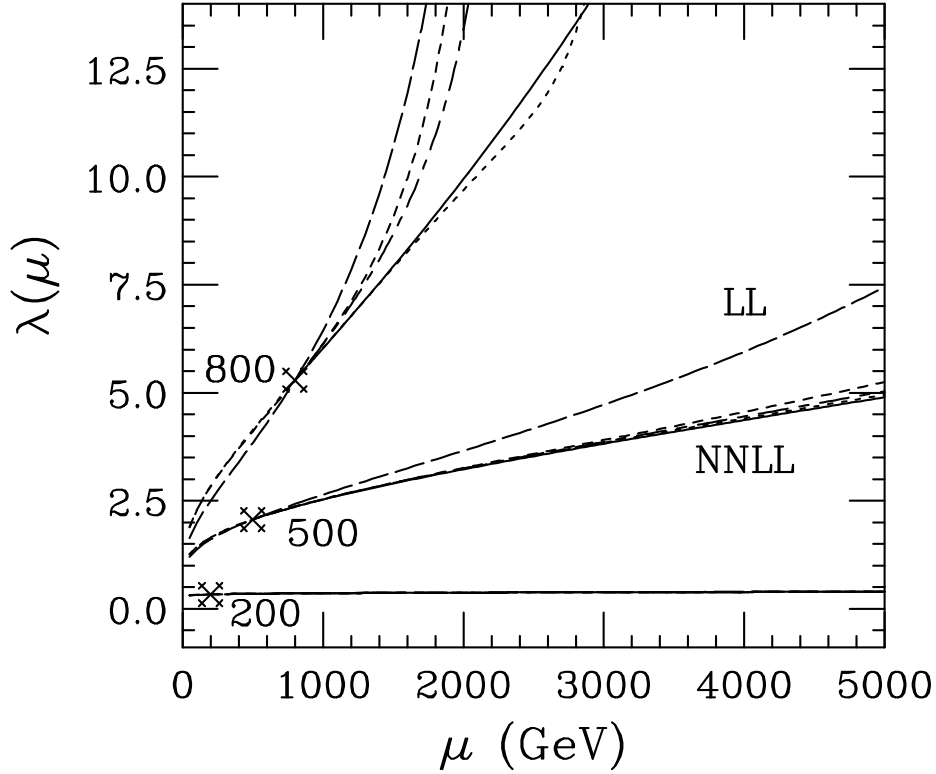


FIG. 3. Different solutions of the three-loop RGE equations for the Higgs quartic coupling  $\lambda$ : the NNLL (three-loop) naive solution according to (2.4) (long-short dashes), the NNLL consistent solution of (2.5) (solid line), the NNLL iterative solution (short dashes), and the NNLL QCD-like solution expanded in powers of  $1/\ln(\Lambda_H^2/\mu^2)$  given in (2.7) (dots). The symbols and labels are the same as in Fig. 1. For comparison, the LL (one-loop) solution (long dashes) is shown again.

$M_H$  are of key importance: If the Higgs self-interaction is non-perturbative at the scale  $M_H$  at which (1.1) is imposed, we do not expect perturbation theory to work in any other observable. Two-body Higgs decay rates are examples for such one-scale processes. They do not contain large logarithms, which need to be summed to all orders. Nevertheless as emphasized at the end of Sect. III A, RG methods can be used to judge the accuracy of perturbation theory: The dependence on the renormalization scale  $\mu$ , at which the decay rate is evaluated, is of the neglected order in  $\lambda$ . The stability of the perturbative result with respect to variations of  $\mu$  must therefore increase order-by-order in  $\lambda$ . This criterion to test perturbation theory has been first used in QCD in [15] and has become a standard method in QCD. Likewise the ratio of two results obtained in different renormalization schemes must approach unity with increasing order in  $\lambda$ . This renormalization scheme dependence will be the second tool used in the analysis of the breakdown of perturbation theory.

### A. Higgs decay into gauge bosons

At first we consider the decay rate of a Higgs into two gauge bosons. The  $O(\lambda^n)$  corrections to the decay rate  $H \rightarrow W^+W^-$  are the same as the ones for the decay into two  $Z$  bosons. The

decay rates of the two channels only differ by an overall factor of proportionality.

We write for the decay rate

$$\Gamma(H \rightarrow W^+W^-) = \Gamma_{\text{tree}} \frac{\lambda_{\text{scheme}}}{\lambda_{\text{tree}}} (1 + \Delta\Gamma_{\text{scheme}}). \quad (4.1)$$

Here  $\Gamma_{\text{tree}}$  is the Born approximation with

$$\Gamma_{\text{tree}} = M_H \sqrt{1 - \frac{4M_W^2}{M_H^2}} \left( 1 - \frac{4M_W^2}{M_H^2} + \frac{12M_W^4}{M_H^4} \right) \frac{\lambda_{\text{tree}}}{8\pi}. \quad (4.2)$$

The corrections stemming from the Higgs self-interaction have been calculated in the OMS scheme to two loops [16]:

$$1 + \Delta\Gamma_{\text{OMS}} = 1 + 2.80\hat{\lambda}_{\text{OMS}} + 62.15\hat{\lambda}_{\text{OMS}}^2 + \mathcal{O}(\hat{\lambda}_{\text{OMS}}^3) + \mathcal{O}\left(\frac{M_W^2}{M_H^2}\right). \quad (4.3)$$

In [16] it has been stressed that the two-loop OMS correction exceeds the one-loop OMS term for  $M_H > 930$  GeV, although the one-loop correction is still small compared to the tree-level term. This indicates that either perturbation theory does not work for  $M_H > 930$  GeV or the one-loop term is accidentally small in the OMS scheme.

Using (3.5) we can express  $\Gamma$  in terms of the  $\overline{\text{MS}}$  coupling:

$$\begin{aligned} 1 + \Delta\Gamma_{\overline{\text{MS}}} = 1 - \hat{\lambda}_{\overline{\text{MS}}} \left( 12 \ln \frac{\mu^2}{M_H^2} + 5.88 \right) + \hat{\lambda}_{\overline{\text{MS}}}^2 \left( 144 \ln^2 \frac{\mu^2}{M_H^2} + 297.0 \ln \frac{\mu^2}{M_H^2} - 122.7 \right) \\ + \mathcal{O}(\hat{\lambda}_{\overline{\text{MS}}}^3) + \mathcal{O}\left(\frac{M_W^2}{M_H^2}\right). \end{aligned} \quad (4.4)$$

Here  $\mu$  is the renormalization scale at which the decay rate is evaluated. The renormalization point  $\mu_0$ , at which the coupling is defined by (3.3) in terms of  $G_F$  and  $M_H$ , is chosen as  $\mu_0 = M_H$  throughout this section. If we also take  $\mu = M_H$ , we observe that the apparent convergence of  $\Delta\Gamma_{\overline{\text{MS}}}$  is worse than that of  $\Delta\Gamma_{\text{OMS}}$  since both  $\lambda_{\overline{\text{MS}}} > \lambda_{\text{OMS}}$  and the  $\overline{\text{MS}}$  coefficients of the perturbation series are in magnitude larger than in the OMS scheme. The two-loop  $\overline{\text{MS}}$  correction equals the one-loop  $\overline{\text{MS}}$  term for  $M_H = 770$  GeV. The corresponding OMS result yields  $M_H = 930$  GeV.

Let us now investigate whether one can refine these bounds on a perturbative Higgs mass by the examination of the renormalization scheme and scale dependence.

We start our analysis by looking at the scheme dependence of the decay width. In the left plot of figure Fig. 4 we show the normalized scheme dependence  $(\Gamma_{\text{OMS}} - \Gamma_{\overline{\text{MS}}})/\Gamma_{\text{tree}}$  at one and two loops, using NLL and NNLL running couplings, respectively. The plot indicates that for  $M_H < 469$  GeV the scheme dependence is reduced when going from one-loop to two-loop order. For larger Higgs masses, the scheme dependence increases, suggesting that perturbation theory is not working satisfactory or even fails. The scheme-dependence criterion indicates problems with perturbation theory in at least one of the two schemes considered for  $M_H > 469$  GeV. The criterion, however, is sensitive to the possibility of an accidental smallness of the one-loop correction. We remark here that the two-loop  $\overline{\text{MS}}$  term in (4.4) is less than four times the square of the one-loop term, while in the OMS scheme, (4.3), this ratio almost equals eight. For  $M_H = 700$



GeV the result for  $\Gamma_{\text{OMS}}$  is larger than the  $\overline{\text{MS}}$  expression by 23%, and for  $M_H = 780$  GeV the scheme dependence reaches unacceptable 52%. The simple criterion of comparing the magnitudes of the one-loop and two-loop contributions gives upper bounds on  $M_H$  which seem to be too large.

Another criterion for the validity of perturbation theory is the order-by-order reduction of the scale dependence. The explicit  $\mu$ -dependent logarithms in (4.4) compensate the effect of the running coupling  $\lambda(\mu)$  to the order considered. To use this criterion in the OMS scheme as well, we need to introduce the RG logarithms into the OMS decay width (4.3). In the OMS scheme, the Callan-Symanzik equation describes the response of some Green's function to the scaling  $p_j \rightarrow \mu/M_H \cdot p_j$  of its external momenta. Its solution for the decay rate (4.3) reads

$$\begin{aligned}
1 + \Delta\Gamma_{\text{OMS}} = 1 + \hat{\lambda}_{\text{OMS}}(\mu) & \left( -12 \ln \frac{\mu^2}{M_H^2} + 2.80 \right) \\
& + \hat{\lambda}_{\text{OMS}}^2(\mu) \left( 144 \ln^2 \frac{\mu^2}{M_H^2} + 88.8 \ln \frac{\mu^2}{M_H^2} + 62.15 \right) \\
& + \mathcal{O}(\hat{\lambda}_{\text{OMS}}^3) + \mathcal{O}\left(\frac{M_W^2}{M_H^2}\right). \tag{4.5}
\end{aligned}$$

Expanding the running coupling  $\lambda_{\text{OMS}}(\mu)$  in (4.1) and (4.5) in terms of  $\lambda_{\text{OMS}}(M_H)$ , (4.5) yields (4.3) up to the neglected order  $\lambda_{\text{OMS}}^3$ , of course. The OMS result expressed in terms of the running coupling (4.5) can be used to examine the scale dependence of the decay width.

We use the LL, NLL and NNLL expressions of the decay rates which consist of the Born, one- and two-loop result in (4.4) supplied with the LL, NLL or NNLL running coupling  $\lambda_{\overline{\text{MS}}}(\mu)$ , respectively. Then the renormalization scale  $\mu$  is varied. The right plot in Fig. 4 shows that perturbation theory nicely works for the  $\overline{\text{MS}}$  scheme if  $M_H = 400$  GeV: The scale dependence diminishes order-by-order. A similar behavior is found for the OMS result using the OMS running coupling and the same value of  $M_H$ . Next we look for an upper bound for a perturbative Higgs mass. We investigate the scale dependence of the decay rate for values of  $M_H$  up to 800 GeV. Based on the size of the logarithmic terms in the higher orders of the perturbation series for the  $\lambda_{\overline{\text{MS}}}$  we have already advocated the range  $0.8M_H < \mu < 1.25M_H$  in Sect. III A. We may add a physical argument for this range as well: Suppose one decides to include the non-zero width of the Higgs into the analysis. Then the decay diagrams must be calculated with an off-shell Higgs boson with invariant mass  $\sqrt{s}$ , and the result is convoluted with a Breit-Wigner function. The decay rate would differ from (4.4) by a function of  $s$  and  $M_H$  vanishing for  $s = M_H^2$ . The decay rate then involves two logarithms:  $\ln(\mu^2/s)$  and  $\ln(\mu^2/M_H^2)$ . The choice of  $\mu$  could be with equal right  $\mu = M_H$ ,  $\mu = \sqrt{s}$  or any scale in between. This suggests choosing the range for  $\mu$  to be of the order of the total width. For the values of Higgs masses we are interested in, the width is between  $0.2M_H$  and  $0.3M_H$  [16], so that the range  $0.8M_H < \mu < 1.25M_H$  is appropriate in both OMS and  $\overline{\text{MS}}$  scheme.

In Fig. 5 we have plotted the scale dependence of  $\Gamma(H \rightarrow W^+W^-)/(\Gamma_{\text{tree}})$  vs. the physical Higgs mass in both OMS and  $\overline{\text{MS}}$  scheme. The tree-level coupling is  $\lambda_{\text{tree}} = G_F M_H^2 / \sqrt{2}$ . The scale dependence at a given order is represented by the smallest and the largest value of  $\Gamma/\Gamma_{\text{tree}}$  when  $\mu$  is varied in the range  $0.8M_H \leq \mu \leq 1.25M_H$ . In the  $\overline{\text{MS}}$  scheme the scale dependence correctly decreases when passing from LL to NLL to NNLL order if  $M_H < 742$  GeV. For  $M_H = 742$  GeV the scale dependence in the LL and NLL order become equal and reach 36%. For  $M_H > 750$  GeV and  $\mu = 1.25M_H$ , the consistent solution of the NNLL running coupling is no

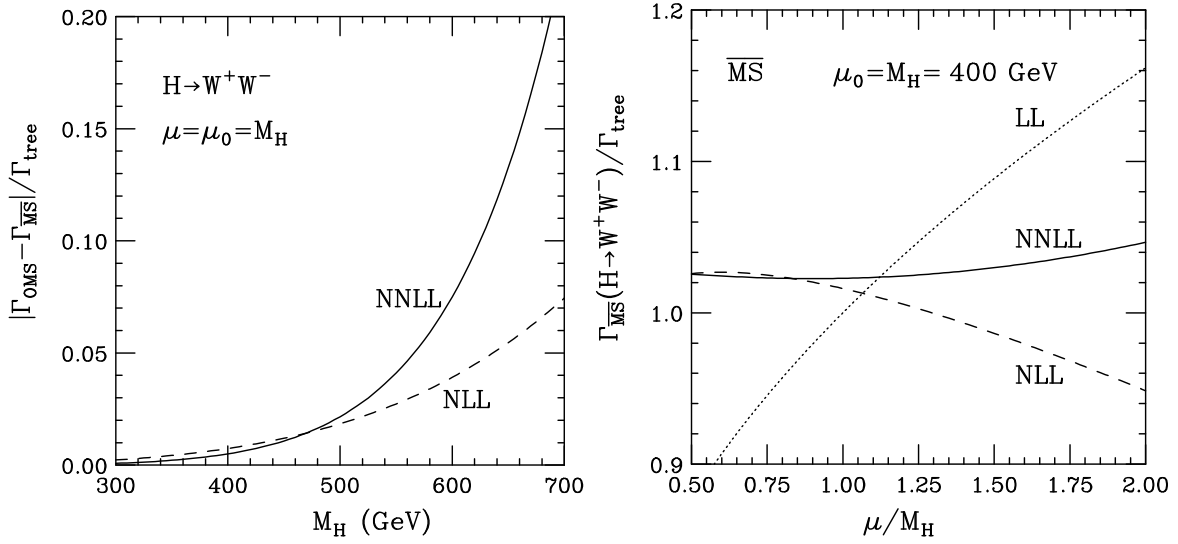


FIG. 4. The left plot shows the scheme dependence  $(\Gamma_{\text{OMS}} - \Gamma_{\overline{\text{MS}}})/\Gamma_{\text{tree}}$  of the decay rate  $\Gamma(H \rightarrow W^+W^-)$ . For  $M_H > 469$  GeV the two-loop scheme dependence (solid line) is larger than the one-loop scheme dependence (dashed). The right plot shows the dependence on the renormalization scale  $\mu$  of  $\Gamma_{\overline{\text{MS}}}$  for  $M_H = 400$  GeV. The scale dependence diminishes sizably order-by-order indicating that perturbation theory works well for this value of  $M_H$ .

longer defined in the  $\overline{\text{MS}}$  scheme, indicating the ultimate breakdown. In the OMS scheme, the NLL and NNLL scale dependences become equal for  $M_H = 672$  GeV, but are numerically small (8%).

We conclude that perturbation theory for bosonic Higgs decays breaks down for Higgs masses of the order of 700 GeV. The scale-dependence criterion yields similar upper bounds on  $M_H$  in both schemes, although the absolute scale dependence is much smaller in the OMS scheme than in the  $\overline{\text{MS}}$  scheme. Using running coupling solutions other than the consistent one (2.5), we obtain similar bounds.

It should be noted that our scale-dependence criterion is not only sensitive to the coefficients of the different orders in  $\Delta\Gamma$ , but also to the coefficients of the  $\beta$ -functions which also enter the non-logarithmic terms of the uncalculated higher orders via diagrams connected with counterterms in (3.1).

## B. Higgs decay into two fermions

Our next example is the fermionic decay width of the Higgs particle. At Born level it reads

$$\Gamma_{\text{tree}}(H \rightarrow f\bar{f}) = \frac{N_c m_f^2 M_H}{8\pi v^2} \left(1 - \frac{4m_f^2}{M_H^2}\right)^{3/2}. \quad (4.6)$$

Here  $N_c = 1$  (3) for lepton (quark) flavors. At tree level, this process is independent of the Higgs coupling  $\lambda$ . Including radiative corrections, the fermionic decay rate receives corrections in powers of  $\lambda$ . In the OMS scheme they are [9,17]

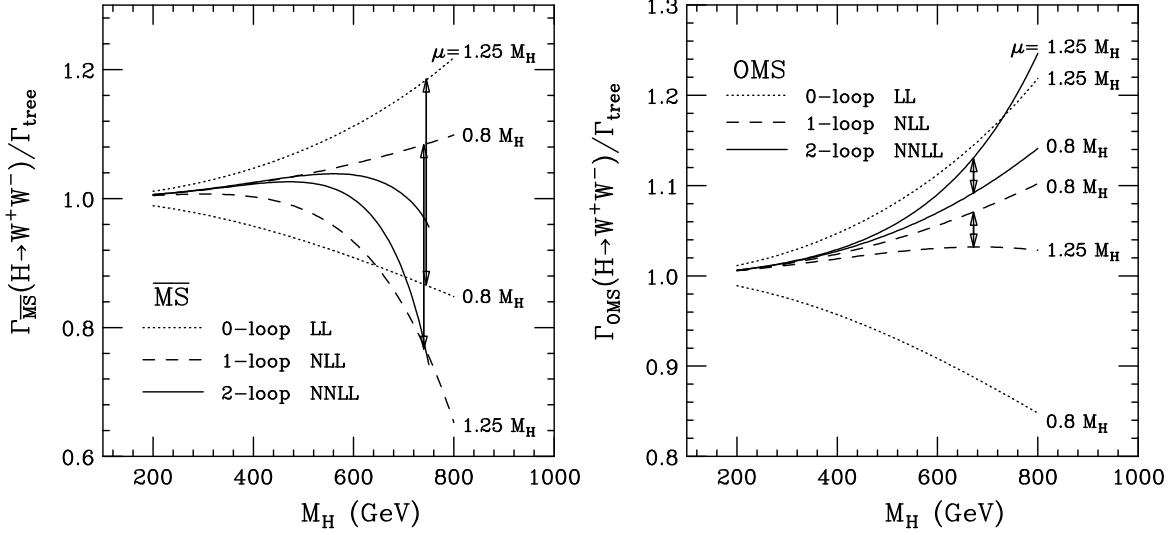


FIG. 5. The scale dependence of  $\Gamma/\Gamma_{\text{tree}}$  for  $H \rightarrow W^+W^-$  in the  $\overline{\text{MS}}$  (left plot) and OMS (right plot) scheme. The extremal values of  $\Gamma/\Gamma_{\text{tree}}$  are plotted for  $0.8M_H \leq \mu \leq 1.25M_H$  in the LL (dotted), NLL (dashed) and NNLL (solid) approximation. Except for the  $\overline{\text{MS}}$  NNLL solution the extremal values correspond to the chosen bounds  $\mu = 0.8M_H$  and  $\mu = 1.25M_H$  as indicated in the figures. The scale dependence diminishes order-by-order for  $M_H < 742$  GeV in the  $\overline{\text{MS}}$  scheme and for  $M_H < 672$  GeV in the OMS scheme. The arrows indicate the equality of the LL and NLL scale uncertainty in the  $\overline{\text{MS}}$  scheme (left plot), and the equality of NLL and NNLL scale uncertainty in the OMS scheme (right plot).

$$1 + \Delta\Gamma_{\text{OMS}}(H \rightarrow f\bar{f}) \approx 1 + 2.12\hat{\lambda}_{\text{OMS}} - 32.66\hat{\lambda}_{\text{OMS}}^2 + \mathcal{O}(\hat{\lambda}_{\text{OMS}}^3). \quad (4.7)$$

Since the tree-level result of the fermionic Higgs decay, Eq. (4.6), is independent of the coupling  $\lambda$ , we only need the one-loop relation between  $\lambda_{\text{OMS}}$  and  $\lambda_{\overline{\text{MS}}}$  to calculate the  $\overline{\text{MS}}$  decay width up to two loops. Likewise, our scale variation criterion only involves LL and NLL running coupling in connection with the one-loop and two-loop results. As a result we can only compare the scale dependence of two instead of three orders. Since the LL one-loop result is identical in both schemes, the scheme dependence can only be compared at the NLL two-loop level. No bounds on  $M_H$  can be derived from the scheme-dependence criterion without knowing the three-loop corrections. This distinguishes the decay  $\Gamma(H \rightarrow f\bar{f})$  from the case  $\Gamma(H \rightarrow W^+W^-)$  discussed in the preceeding section.

Combining Eq. (3.3) with the previous equation, we obtain the correction to the fermionic Higgs decay in  $\overline{\text{MS}}$  quantities [18,19]:

$$1 + \Delta\Gamma_{\overline{\text{MS}}}(H \rightarrow f\bar{f}) \approx 1 + 2.12\hat{\lambda}_{\overline{\text{MS}}} - (51.03 + 25.41 \ln(\mu^2/M_H^2)) \hat{\lambda}_{\overline{\text{MS}}}^2 + \mathcal{O}(\hat{\lambda}_{\overline{\text{MS}}}^3). \quad (4.8)$$

We also give the scale dependence of the OMS result:

$$1 + \Delta\Gamma_{\text{OMS}} = 1 + 2.12\hat{\lambda}_{\text{OMS}}(\mu) - \left(32.66 + 25.41 \ln \frac{\mu^2}{M_H^2}\right) \hat{\lambda}_{\text{OMS}}(\mu) + \mathcal{O}(\hat{\lambda}_{\text{OMS}}^3). \quad (4.9)$$

In Fig. 6 we show the scale dependence of the decay width expressed in terms of the running coupling in both  $\overline{\text{MS}}$  and OMS scheme at one and two loops as a function of  $M_H$ . At each order

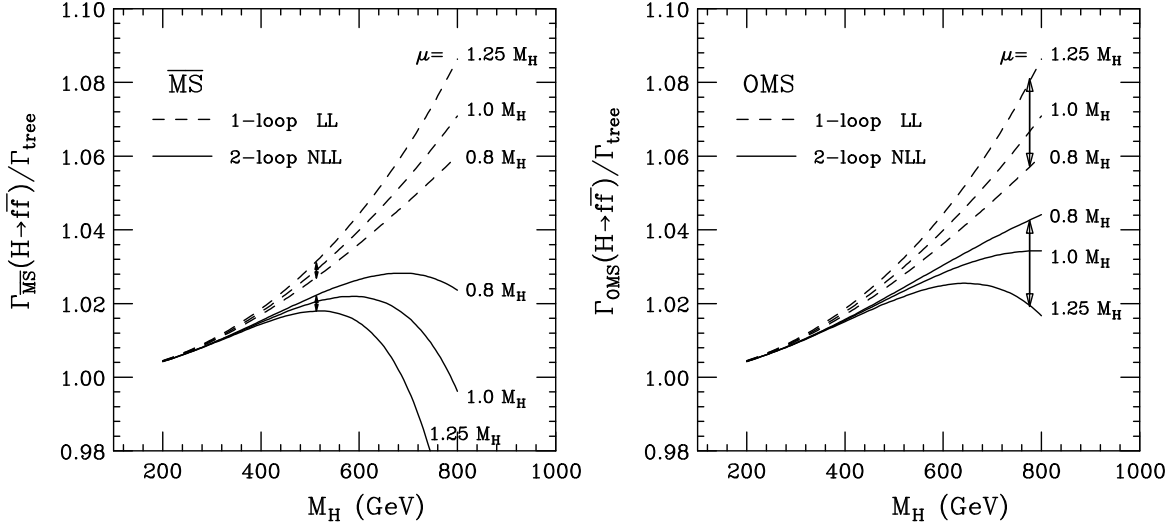


FIG. 6. The resummed  $\mu$ -dependence of the normalized fermionic Higgs decay width. Only the  $\mu$ -dependence entering through the Higgs coupling is analyzed, i.e. no running Yukawa or QCD couplings are considered. Using the  $\overline{\text{MS}}$  renormalization scheme (left plot), the  $\mu$ -dependence of the 2-loop result is as big as the  $\mu$ -dependence of the 1-loop result for  $M_H = 513$  GeV as indicated by arrows. In the OMS, this equality occurs for  $M_H = 776$  GeV (right plot). The scale dependence is nevertheless small at these critical Higgs mass values.

the three curves refer to  $\mu = 0.8M_H$ ,  $1.0M_H$ , and  $1.25M_H$ . We find that the  $\mu$  dependence of the two-loop result is larger than the  $\mu$  dependence of the one-loop result if  $M_H$  is larger than 513 GeV in the  $\overline{\text{MS}}$  scheme. In the OMS scheme the corresponding bound is  $M_H = 776$  GeV. These results, however, are not as valuable as those found in the previous section, since they are only founded on the comparison of two orders rather than three. The low value of  $M_H = 513$  GeV in the  $\overline{\text{MS}}$  scheme may be accidental. The scale dependence is very weak, less than a few percent for Higgs masses up to 750 GeV. This is due to the fact that the tree-level result does not depend on  $\lambda$ . The scheme dependence at NLL (two-loop) is marginal for the same reason. We presently have no information on the NNLL behaviour of the fermionic decay. Looking at Fig. 6 we conclude that the upper bound on a perturbative Higgs mass is in agreement with our findings in the case of the bosonic Higgs decay.

## V. SCHEME AND SCALE DEPENDENCE OF CROSS SECTIONS

The previous section considered one-scale processes. The only logarithms appearing in the RG improved results are  $\ln(\mu^2/M_H^2)$ . Testing the perturbativity of Higgs sector is much more stringent when considering high-energy two-scale processes, because they involve the running coupling at a high scale. Typical two-scale processes which depend on the coupling  $\lambda$  are  $2 \rightarrow 2$  scattering processes involving longitudinally polarized gauge bosons and the Higgs boson. In the limit  $s, M_H^2 \gg M_W^2$  the longitudinally polarized gauge bosons can be replaced by massless Goldstone bosons. In this limit all couplings except for the trilinear and quartic Higgs coupling are subleading and can be neglected. Also assuming  $s \gg M_H^2$ , the high-energy amplitudes and

cross sections have been calculated to two loops by [8,20]. The high-energy limit is approached if  $\sqrt{s} > 2M_H$  [20]. Its error is less than a few percent if  $\sqrt{s} > 5M_H$ . For most of our analysis we will consider  $\sqrt{s} = 2$  TeV.

A typical example is the process  $W_L^+ W_L^- \rightarrow Z_L Z_L$ . The high-energy cross section only depends on  $\sqrt{s}$ ,  $M_H$ , and  $\lambda$ . The OMS cross section is [20]

$$\begin{aligned} \sigma(s) = \frac{1}{8\pi s} [\lambda_{\text{OMS}}(\mu)]^2 & \left[ 1 + \left( 24 \ln \frac{s}{\mu^2} - 42.65 \right) \frac{\lambda_{\text{OMS}}(\mu)}{16\pi^2} \right. \\ & + \left( 432 \ln^2 \frac{s}{\mu^2} - 1823.3 \ln \frac{s}{\mu^2} + 24.0 \ln \frac{s}{M_H^2} + 2455.1 \right) \frac{[\lambda_{\text{OMS}}(\mu)]^2}{(16\pi^2)^2} \\ & \left. + \mathcal{O}([\lambda_{\text{OMS}}(\mu)]^3) \right], \end{aligned} \quad (5.1)$$

where the OMS renormalization fixes  $\mu_0 = M_H$  such that the OMS running coupling has the boundary condition  $\lambda_{\text{OMS}}(\mu = \mu_0) = M_H^2/(2v^2)$ . The scale  $\mu$  must be chosen of the order  $\sqrt{s}$  to resum the large logarithms to all orders. For a complete resummation of all logarithms up to three loops, one uses the NNLL running coupling and takes  $\mu = \sqrt{s}$ . The  $\mu$ -independent logarithm is related to the field anomalous dimension and needs no resummation because of the smallness of its coefficient. At one loop, the anomalous dimensions of the Higgs and gauge bosons are zero, and at two loops they are numerically unimportant [8].

The  $\overline{\text{MS}}$  result is

$$\begin{aligned} \sigma(s) = \frac{1}{8\pi s} [\lambda_{\overline{\text{MS}}}(\mu)]^2 & \left[ 1 + \left( 24 \ln \frac{s}{\mu^2} - 60.0 \right) \frac{\lambda_{\overline{\text{MS}}}(\mu)}{16\pi^2} \right. \\ & + \left( 432 \ln^2 \frac{s}{\mu^2} - 2472.0 \ln \frac{s}{\mu^2} + 24.0 \ln \frac{s}{M_H^2} + 3367.9 \right) \frac{[\lambda_{\overline{\text{MS}}}(\mu)]^2}{(16\pi^2)^2} \\ & \left. + \mathcal{O}([\lambda_{\overline{\text{MS}}}(\mu)]^3) \right]. \end{aligned} \quad (5.2)$$

We choose the renormalization point to be  $\mu_0 = M_H$  such that the the  $\overline{\text{MS}}$  running coupling is fixed at  $\mu = \mu_0$  by (3.3).

The RG structure of the cross section is similar to the one of the decay width  $\Gamma(H \rightarrow W^+ W^-)$  since the tree-level result also depends on  $\lambda$ . There are two important differences: the tree-level cross section is proportional to  $\lambda$  *squared*, and the running coupling resums terms of order  $\ln(s/M_H^2)$  which can lead to a significant increase of the running coupling compared to the tree-level coupling.

### A. Perturbativity at collider energies

Choosing  $\mu = \sqrt{s} = 2000$  GeV, we show the scheme dependence of the cross section  $W_L^+ W_L^- \rightarrow Z_L Z_L$  in Fig. 7. For Higgs masses larger than 400 GeV, the scheme dependence is larger than 40% and actually increases when going from NLL to NNLL cross section. Choosing  $\mu = \sqrt{s} = 1000$  GeV, a value more realistic for  $WW$ -scattering at future colliders, we find the critical mass value to be  $M_H = 436$  GeV. For such values of  $M_H$  and  $\sqrt{s}$  the high-energy approximation yields about 70% of the exact  $\lambda$ -dependence of the cross section [20]. Increasing  $\sqrt{s}$ , the

breakdown of perturbation theory as seen in the scheme-dependence criterion happens for smaller and smaller values of  $M_H$ . We will come back to this later.

In addition to the scheme dependence, we also evaluate the scale-dependence criterion. Since the renormalization group is used to resum  $\ln(s)$  terms, the scale  $\mu$  is varied around  $\sqrt{s}$  rather than  $M_H$ . The arguments of Sect. III, which are based on the size of the beta function coefficients, suggest the range  $0.8\sqrt{s} < \mu < 1.25\sqrt{s}$ . Choosing  $\sqrt{s} = 2000$  GeV, the result of this variation is shown in Fig. 8 for both  $\overline{\text{MS}}$  and OMS scheme. In the  $\overline{\text{MS}}$  scheme, we observe a nice order-by-order reduction of the scale dependence if  $M_H$  is less than 357 GeV. For larger values of  $M_H$ , the NLL scale dependence exceeds the LL one, and for  $M_H > 368$  GeV we also find the NNLL scale dependence to be larger than the NLL one. For the OMS result we find only one crossing point. There the NNLL scale dependence dominates over the NLL one if  $M_H > 410$  GeV. Taking also the scheme dependence into account we conclude that perturbative results for longitudinal gauge boson scattering at  $\sqrt{s} = 2000$  GeV cease to be meaningful if  $M_H$  is of the order 400 GeV or above. For a value of  $\sqrt{s} = 1000$  GeV we find limits of  $O(450 \text{ GeV})$ , but here the additional low-energy contributions — though not dominant — may change the limit.

The upper bounds on a perturbative Higgs mass from scattering processes are more stringent than the results found in Higgs decays. The reasons are two-fold. First, the one-loop and two-loop coefficients of the perturbative corrections to the cross section are an order of magnitude larger than the corresponding coefficients of the decay processes. Second, the running coupling evaluated at a scale  $\sqrt{s} > M_H$  is numerically larger than the coupling involved in the decay widths.

It is also interesting to note that the bounds derived here are similar to the results found in [21] which are based on perturbative violation of unitarity at two loops, a rather different criterion for the breakdown of perturbation theory. Compared to the nonperturbative lattice results of  $M_H < 710 \pm 60$  GeV [22], our perturbative criteria require smaller Higgs masses.

## B. Perturbativity at large embedding scales

In Fig. 9 we show the upper bound for a perturbative Higgs mass as a function of some embedding scale  $\Lambda$ . Since the Standard Model Higgs sector is — depending on the value of  $M_H$  — not defined above a certain energy scale, it is a common procedure to introduce an embedding scale above which the physical interactions are to be described by a more complete theory. Requiring that the SM Higgs sector is still perturbative at such an embedding scale, it is possible to give upper bounds on the Higgs mass as a function of the embedding scale. Here we require the process  $W_L^+ W_L^- \rightarrow Z_L Z_L$  to be perturbative for energies  $\sqrt{s} \leq \Lambda_{\text{embed}}$  and apply our criteria for scheme and scale dependence to calculate the upper bound on  $M_H$ . The result is shown in Fig. 9. At 2 TeV, the different bounds on  $M_H$  correspond to the values derived from Figs. 7 and 8. For increasing embedding scale, the upper bound on  $M_H$  decreases, and the three different criteria give converging bounds. At  $\Lambda_{\text{embed}} = 10^{16}$  GeV, the upper bound is  $150 \pm 3$  GeV. For such low Higgs masses, however, one expects the top-quark Yukawa coupling to have an influence on the RG evolution of the Higgs coupling. As a matter of fact, the SM beta function of the Higgs coupling can become negative if the Higgs particle is too light, invalidating our analysis. Taking  $m_t = 175$  GeV, this is expected to happen for  $M_H < 135$  GeV [23], which is lower than the values considered by us. Using the results of Lindner [24], we expect the change of our Higgs mass bounds due to a top-quark mass of 175 GeV to be less than 10% for the whole range of energy-scales considered. For

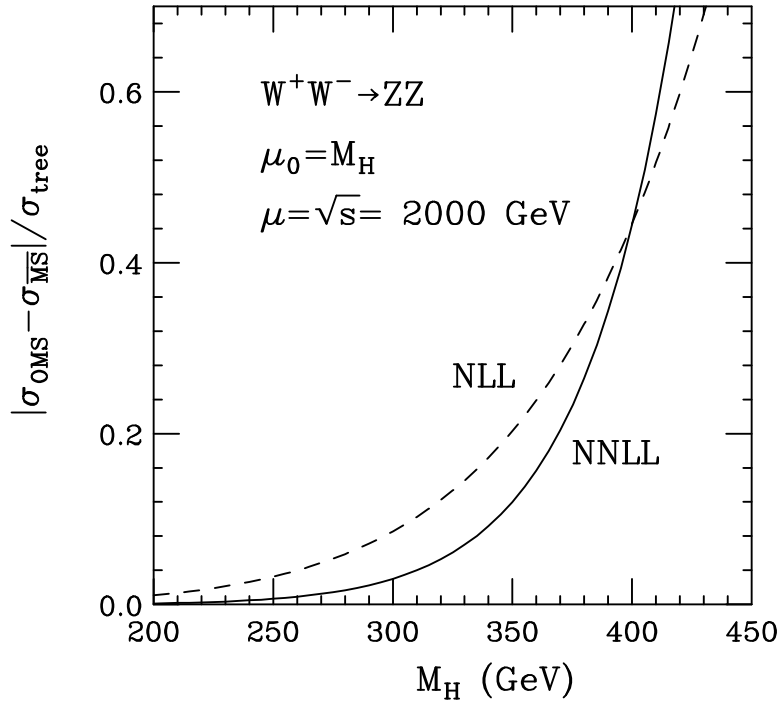


FIG. 7. The scheme dependence of the cross section  $W_L^+ W_L^- \rightarrow Z_L Z_L$  at  $\sqrt{s} = 2$  TeV. For  $M_H > 400$  GeV the two-loop scheme dependence (solid line) is larger than the one-loop scheme dependence (dashed) and exceeds 40%.

comparison, we also display the values of  $M_H$  which would lead to a one-loop Landau singularity at  $\Lambda_{\text{embed}}$ . Calculating the Landau pole, we again neglected Yukawa and gauge couplings.

It is worth noting that our criteria for an upper Higgs mass lead to values of the running coupling at the embedding scale which are not very large. For values of  $\sqrt{s}$  in the TeV range, the maximal allowed value of the running coupling is less than 2.2, and at GUT energies we find the maximal value to be less than 1.6. These small values are surprising: The beta function and the solutions for the running coupling show excellent convergence for such small values. As a matter of fact, the usual criteria for the breakdown of perturbation theory assume that the running coupling becomes large. Yet this method is unsatisfactory: The consideration of the one-loop Landau pole as in [24] cannot be extended to higher orders. Instead the authors of [6] use the criterion of (in our notation)  $\lambda(\Lambda_{\text{embed}}) < \pi^2$ . Here the choice of the numerical bound involves some arbitrariness. The plots in Fig. 1 and Fig. 3 show that  $\pi^2$  is clearly chosen too large, because the different solutions differ substantially for  $\lambda = \pi^2$ . The second arbitrariness of this method resides in the fact that the breakdown of perturbation theory is judged from a scheme dependent quantity:  $\lambda(\Lambda_{\text{embed}})$  depends on the renormalization scheme through the radiative corrections to the matching condition (1.1) and, most important, through the coefficients  $\beta_n$ ,  $n \geq 2$ , of the  $\beta$ -function. In contrast physical observables are scheme independent up to the calculated order. They, however, seem to become non-perturbative for much smaller values of  $\lambda$ . For comparison, the unitarity arguments used in [21] yield an upper bound on the running coupling of 2.3, independent of any choice of  $\sqrt{s}$ .

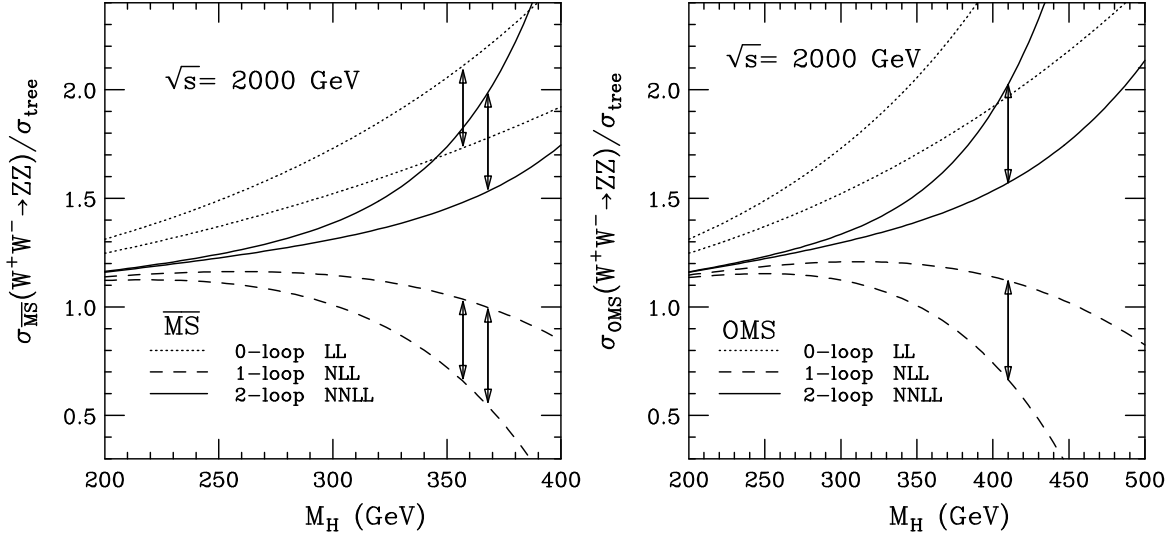


FIG. 8. The resummed  $\mu$ -dependence of the normalized  $W_L^+ W_L^- \rightarrow Z_L Z_L$  cross section at  $\sqrt{s} = 2$  TeV. Only the  $\mu$ -dependence entering through the Higgs coupling is analyzed, i.e. no running Yukawa or QCD couplings are considered. Using the  $\overline{\text{MS}}$  renormalization scheme, only a Higgs mass of less than 357 GeV guarantees an order-by-order reduction of the scale dependence. In the OMS scheme, the NLL and NNLL are equal if  $M_H = 410$  GeV. The scale dependence is almost 50% at this value of  $M_H$ .

## VI. CONCLUSIONS

Our analysis of various physical processes of the Higgs sector indicates that the breakdown of perturbation theory cannot be judged purely on grounds of a large Higgs (running) coupling. The breakdown of perturbation theory in both Higgs decays ( $\lambda_{\text{OMS}} = G_F M_H^2 / \sqrt{2} < 4$ ) and scattering processes ( $\lambda(\sqrt{s}) < 2.2$ ) occurs for relatively small values of the Higgs coupling. The usual criterion — the breakdown of the perturbative behaviour of the beta function and the running coupling — yields upper bounds for a perturbative Higgs mass which are too large.

Applying our criteria of scheme-dependence and scale-dependence to Higgs decays, we find a satisfactory perturbative behaviour of the decay widths if  $M_H < \text{O}(700 \text{ GeV})$ . In the case of  $2 \rightarrow 2$  scattering processes, one needs to specify the energy scale at which the process is to take place. Choosing  $\sqrt{s}$  to be a couple of TeV, the Higgs mass has to be less than  $\text{O}(400 \text{ GeV})$  to guarantee a good perturbative behaviour of the cross section for  $W_L^+ W_L^- \rightarrow Z_L Z_L$  scattering. Requiring such processes to be perturbative at  $\sqrt{s} = 10^{16} \text{ GeV}$ , the Higgs mass has to be less than  $\text{O}(150 \text{ GeV})$ .

## VII. ACKNOWLEDGMENTS

One of the authors (K.R.) gratefully acknowledges the hospitality of the Aspen Center for Physics where parts of this work were done, and thanks M. Lindner and S. Willenbrock for interesting and informative discussions.



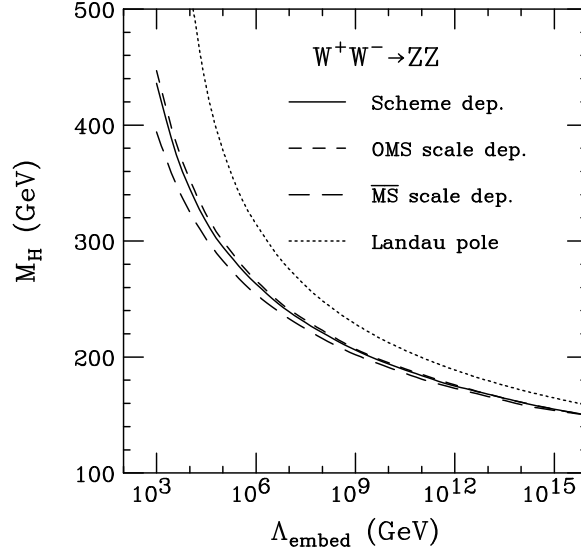


FIG. 9. Upper bound on  $M_H$  derived using our scheme-dependence and scale-dependence criteria. We require the SM process  $W_L^+ W_L^- \rightarrow Z_L Z_L$  to remain perturbative for cms-energies up to  $\sqrt{s} = \Lambda_{\text{embed}}$ . For comparison we also show the values of  $M_H$  which lead to a Landau singularity in the one-loop running coupling at the scale  $\mu = \Lambda_{\text{embed}}$ .

## REFERENCES

- [1] I. Jack and H. Osborn, J. Phys. **A16**, 1101 (1983).
- [2] E. Lendvai, G. Pócsik, and T. Torma, Mod. Phys. Lett. A **6**, 1195 (1991); Acta Phys. Pol. B **22**, 607 (1991).
- [3] W. A. Bardeen, A. J. Buras, D. W. Duke and T. Muta, Phys. Rev. **D18**, 3998 (1978).
- [4] L.D. Landau, in : Niels Bohr and the development of physics (McGraw-Hill, New York, 1955).
- [5] L. Maiani, G. Parisi, and R. Petronzio, Nucl. Phys. **B136**, 115 (1979);  
N. Cabbibo, L. Maiani, G. Parisi, and R. Petronzio, Nucl. Phys. **B158**, 295 (1979).
- [6] B. Grzadkowski and M. Lindner, Phys. Lett. **B178**, 81 (1986).
- [7] In the context of lattice studies this has been discussed in: M. Lüscher and P. Weisz, Phys. Lett. **B212**, 472 (1988).
- [8] P.N. Maher, L. Durand, and K. Riesselmann, Phys. Rev. D **48**, 1061 (1993); (E) **52**, 553 (1995);  
A. Ghinculov and J. van der Bij, Nucl. Phys. **B436**, 30 (1995).
- [9] A. Ghinculov, Phys. Lett. B **337**, 137 (1994); (E) **346**, 426 (1994).
- [10] A. Sirlin and R. Zucchini, Nucl. Phys. **B266**, 389 (1986).
- [11] P. Stevenson, Phys. Rev. **D23**, 2916 (1981); Nucl. Phys. **B203**, 472 (1982).
- [12] J.C. Collins, *Renormalization* (Cambridge University Press, Cambridge, 1984), Chap. 9.
- [13] A.A. Vladimirov, D.I. Kazakov, and O.V. Tarasov, Sov. Phys. JETP **50**, 521 (1979).
- [14] M. Lüscher and P. Weisz, Nucl. Phys. **B318**, 705 (1989).
- [15] A. J. Buras, M. Jamin and P. H. Weisz, Nucl. Phys. **B347**, 491 (1990).
- [16] A. Ghinculov, Univ. Freiburg preprint THEP 95/11, hep-ph/9507240.

- [17] L. Durand, B.A. Kniehl, and K. Riesselmann, Phys. Rev. Lett. **72**, 2534 (1994); (E) **74**, 1699 (1995); Phys. Rev. D **51**, 5007 (1995).
- [18] A.I. Bochkarev and R.S. Willey, Phys. Rev. D **51**, 2049 (1995); Eq. (17) of this paper uses incorrect numbers.
- [19] K. Riesselmann, in: Proceedings of the Ringberg Workshop on “Perspectives for electroweak interactions in  $e^+e^-$  collisions”, Munich, Germany (Feb. 5-8, 1995), ed.: B. Kniehl, (World Scientific, Singapore, 1995), p. 175.
- [20] K. Riesselmann, Tech. Univ. Munich preprint TUM-HEP-223/95 (July 1995), hep-ph/9507413.
- [21] L. Durand, P. Maher, and K. Riesselmann, Phys. Rev. D **48**, 1084 (1993).
- [22] U. Heller, M. Klomfass, H. Neuberger, and P. Vranas, Nucl. Phys. **B405**, 555 (1993).
- [23] G. Altarelli and G. Isidori, Phys. Lett. **B337**, 141 (1994).
- [24] M. Lindner, Z. Phys. **C31**, 295 (1986).